JOC The Journal of Organic Chemistry

pubs.acs.org/joc Article

Photoinduced DNA Interstrand Cross-Linking by Benzene Derivatives: Leaving Groups Determine the Efficiency of the Cross-Linker

Heli Fan and Xiaohua Peng*

Cite This: https://dx.doi.org/10.1021/acs.joc.0c02234 Read Online

ACCESS | Metrics & More | Article Recommendations | Supporting Information

ABSTRACT: We have synthesized and characterized two small libraries of 2-OMe or 2-NO_2-benzene analogues **2a−i** and **3a−i** containing a wide variety of leaving groups. Irradiation of these compounds at 350 nm generated benzyl radicals that were spontaneously oxidized to benzyl cations directly producing DNA interstrand cross-links (ICLs). Compounds with a 2-methoxy substituent showed a faster cross-linking reaction rate and higher ICL efficiency than the corresponding 2-nitro analogues. Apart from the aromatic substituent, the benzylic leaving groups greatly affected DNA cross-linking efficiency. Higher ICL yields were observed for compounds with OCH_3 (**3b**), OCH_2Ph (**3d**), or Ph_3P^+ (**3i**) as leaving groups than those containing OAc (**3a**), NMe_2 (**3e**), morpholine (**3f**), $OCH_2CH{=}CH_2$ (**3c**), SPh (**3g**), or SePh (**3h**). The heat stability study of the isolated ICL products indicated that dGs were the preferred alkylation sites in DNA for the benzyl cations produced from **2a−i**, **3c**, and **3e−i** while **3a** (L = OAc), **3b** (L = OMe), and **3d** (L = OCH_2Ph) showed a similar photoreactivity toward dGs and dAs. Although the photogenerated benzyl cations alkylated dG, dC, and dA, ICL assay with variation of DNA sequences showed that the ICL reaction occurred with opposing dG/dC but not with staggered dA/dA.

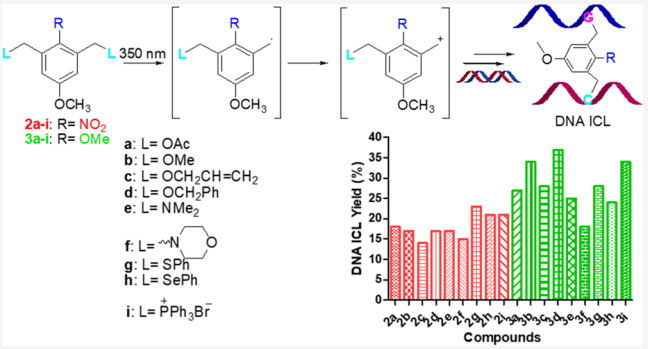

INTRODUCTION

DNA interstrand cross-links (ICLs) prevent the separation of two DNA strands, which inhibits DNA replication, transcription, and any other processes for gene expression. Some chemical reagents directly produce DNA ICLs, such as nitrogen mustards, aldehydes/dialdehydes, and disulfonates, while others have masked but inducible DNA cross-liking capability. Chemical agents capable of inducing ICLs showed wide applications in molecular biology and human medicine. They have been used as anticancer agents[1−4] for DNA damage and repair studies,[5−7] for nucleic acid detection,[8−10] etc. Several methods have been developed for inducing ICL formation, including photoirradiation,[11−16] $NaIO_4$[15,17] or NBS[18,19] oxidation, fluoride induction,[20−22] and H_2O_2 induction.[23,24] Among these methods, photoinduction attracted attention for its biocompatibility and orthogonality. Photoirradiation is clean and non-invasive and does not require additional chemical reagents. Various photoinducible DNA cross-linking agents have been developed to form ICLs. In general, three common mechanisms are involved in a photoinduced ICL formation process, including photocycloadditon, alkylation via quinone methides (QMs), or alkylation via carbocations.[25] The photoinduced DNA ICL formation via photocycloaddition and QM formation has been extensively studied. For instance, psoralens,[26,27] *p*-stibaolze,[28] coumarins,[29,30] 3-cyanovinylcarbazole,[31,32] and furan moiety[33] can induce DNA ICL formation via photocycloaddition, while phenol,[14] biphenol,[14] binol,[11,13,34] or naphthoquinone analogues[35,36] produce DNA ICL products through photogenerated QMs. However, photoinduced DNA ICL formation via carbocation mechanism was less explored until recently. The research groups of Li[37] and Greenberg[38] demonstrated that although photoirradiation of the modified thymidines generated both the free radicals and cations, only the cation intermediates produced DNA cross-linking. Peng and coworkers discovered that photoirradiation of bifunctional aromatic compounds produced bis-carbocations directly cross-linking DNA.[16,39] Several classes of bifunctional aromatic compounds have been reported to induce ICL formation via photogenerated carbocations.[4,16,40,41] Both the leaving groups and the aromatic substituents strongly affected the efficiency of

Received: September 16, 2020

https://dx.doi.org/10.1021/acs.joc.0c02234
J. Org. Chem. XXXX, XXX, XXX−XXX

DNA ICL formation as well as the mechanism pathway for DNA cross-linking.[4] In general, two pathways are involved for carbocation formation, either via homolytic cleavage of the C−L bond to form free radicals that are simultaneously transformed to the carbocations directly alkylating DNA (**pathway 1**) or through heterolytic cleavage of the C−L bond to generate carbocations (**pathway 2**). All compounds with bromo as a leaving group induce ICL formation via **pathway 1** upon 350 nm irradiation, while the pathways for DNA ICL formation induced by those containing trimethyl ammonium salts as leaving groups highly depend on the aromatic substituents.[4,16] The ammonium salts with electron-donating substituents (i.e., **1a**) undergo homolytic cleavage of the C−N bond (**pathway 1**), while those with strong withdrawing groups (i.e., **1b**) undergo heterolytic cleavage of the C−N bond (**pathway 2**).

Several research groups have shown that the leaving groups can modulate the efficiency of the photoactivation process as well as the physical chemical properties of the substrates.[13,42−45] The research groups of Rokita and Freccero demonstrated that −OAc, $-NMe_2$ and −morpholine groups were good leaving groups for QM formation.[13,21,35,42] Benzyl ether groups were also reported to be fast-photocleaving groups that can be cleaved within seconds upon UV irradiation.[44] Greenberg's group discovered that phenyl sulfide- and phenyl selenide-modified pyrimidine nucleosides were efficient photoactivated DNA cross-linkers.[38,46,47] A lipophilic cation, triphenylphosphonium group, was also introduced as the most effective way to deliver drugs specifically to the mitochondria, with the expectation of increasing the UV absorption and improving water solubility.[45] However, previous investigation on cation-mediated ICL formation was limited to two types of leaving groups, e.g., Br and the trimethyl ammonium salts (i.e., **1a−d**) (Scheme 1). The goal of this work is to provide a systematic investigation on how the leaving groups affect photochemical generation of carbocation and the subsequent DNA ICL formation. Thus, we designed and synthesized two series of benzene analogues **2a−i** and **3a−i** that contain a wide variety of leaving groups, including OAc, NMe_2, morpholine, OCH_3, $OCH_2CH{=}CH_2$, OCH_2Ph, SPh, SePh, and triphenylphosphonium bromide group.

Scheme 1. Structures of 2a−i and 3a−i (A) and the Mechanism for DNA ICL Formation Induced by 1a (B) and 1b (C)

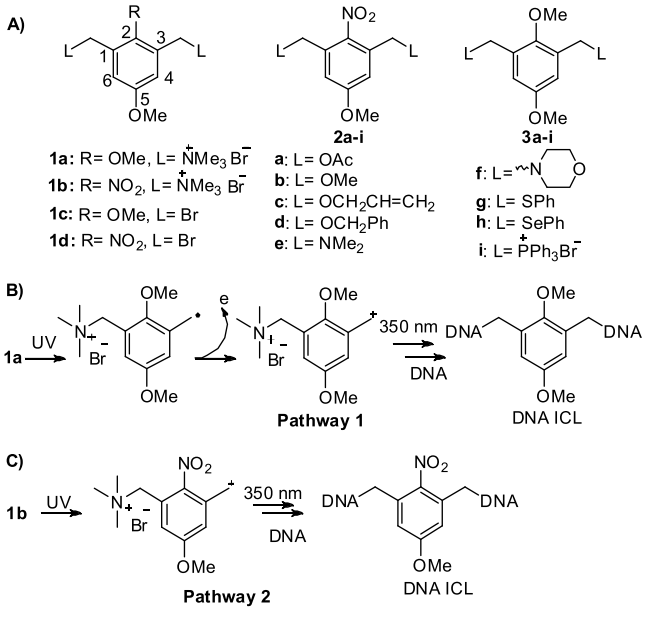

RESULTS AND DISCUSSION

Synthesis. Compounds **2a−d** containing acetate or ether groups were synthesized from diol **4** via nucleophilic substitution reactions while **2e−i** having other leaving groups synthesized from bromide **1d** (Scheme 2). Compounds **1d** and **4** were prepared as previously reported.[4] For the synthesis of **2a−d**, different halides were employed, including acetyl chloride (→**2a**), methyl iodide (→**2b**), allyl iodide (→**2c**), and benzyl bromide (→**2d**) (Scheme 2A). To synthesize **2d**, we initially tried benzyl chloride, but no product was obtained after stirring at rt overnight. Compound **1d** was converted to **2e−i** by treatment with dimethyl amine (→**2e**), morpholine (→**2f**), thiophenol (→**2g**), diphenyl diselenide (→**2h**), or triphenylphosphine (→**2i**) in good or moderate yields (Scheme 2B).

Compounds **3a−i** were synthesized starting from 4-methoxyphenol (**5**) (Scheme 3). Selective hydroxymethylation of **5** at the positions ortho to the hydroxyl group was performed with formaldehyde under basic conditions yielding 4-methoxy-2,6-bis(hydroxymethyl)phenol (**6**) (Scheme 3A). Methylation of **6** with methyl iodide provided (2,5-dimethoxy-1,3-phenylene)dimethanol (**7**) that served as a common precursor for **3a−i**. Compound **7** was converted to **3a−d** by reacting with various halides, such as acetyl chloride (→**3a**), methyl iodide (→**3b**), allyl iodide (→**3c**), and benzyl chloride (→**3d**) (Scheme 3B). Compound **7** was also transformed to **1c** via bromination by PBr_3 resulting in 90% yield, which was higher than that reported by Fan and co-authors (62%) (Scheme 3A).[4] Similar to the synthesis of **2e−i**, compounds **3e−i** were obtained by treatment of **1c** with dimethyl amine (→**3e**), morpholine (→**3f**), thiophenol (→**3g**), diphenyl diselenide (→**3h**), or triphenylphosphine (→**3i**) in good or moderate yields (Scheme 3C).

DNA Interstrand Cross-Linking Assay. Similar to previous studies, a 49-mer DNA duplex (**8**) was used for investigating the photoreactivity of **2a−i** and **3a−i** toward DNA.[4,16] The DNA cross-linking assay was performed in a phosphate buffer (pH 8.0) with 350 nm irradiation. Denaturing polyacrylamide gel electrophoresis (PAGE) was used for DNA ICL analysis. None of these compounds produced DNA ICLs without photoirradiation, while efficient ICL formation was observed for all of them upon 350 nm irradiation. The results suggested that **2a−i** and **3a−i** were efficient photoactivated DNA cross-linkers. To fully understand how the aromatic substituents and leaving groups affect the reactivity of these compounds, we carried out time-dependent DNA cross-link study for **2a−i** and **3a−i** (Table 1 and Figures S1−S18, Supporting Information). Among all compounds tested, those with an electron-donating aromatic substituent (**3a-i**: R = OMe) showed a much faster photoinduced DNA cross-linking reaction rate than the corresponding NO_2-containing compounds **2a−i**. This indicated that electron-donating substituents promoted the reaction rate, while electron-withdrawing groups suppressed this process. This is well correlated with the electron-deficient nature of the carbocation intermediates that are stabilized by the presence of electron-donating groups.

https://dx.doi.org/10.1021/acs.joc.0c02234
J. Org. Chem. XXXX, XXX, XXX−XXX

Scheme 2. Synthesis of 2a−i

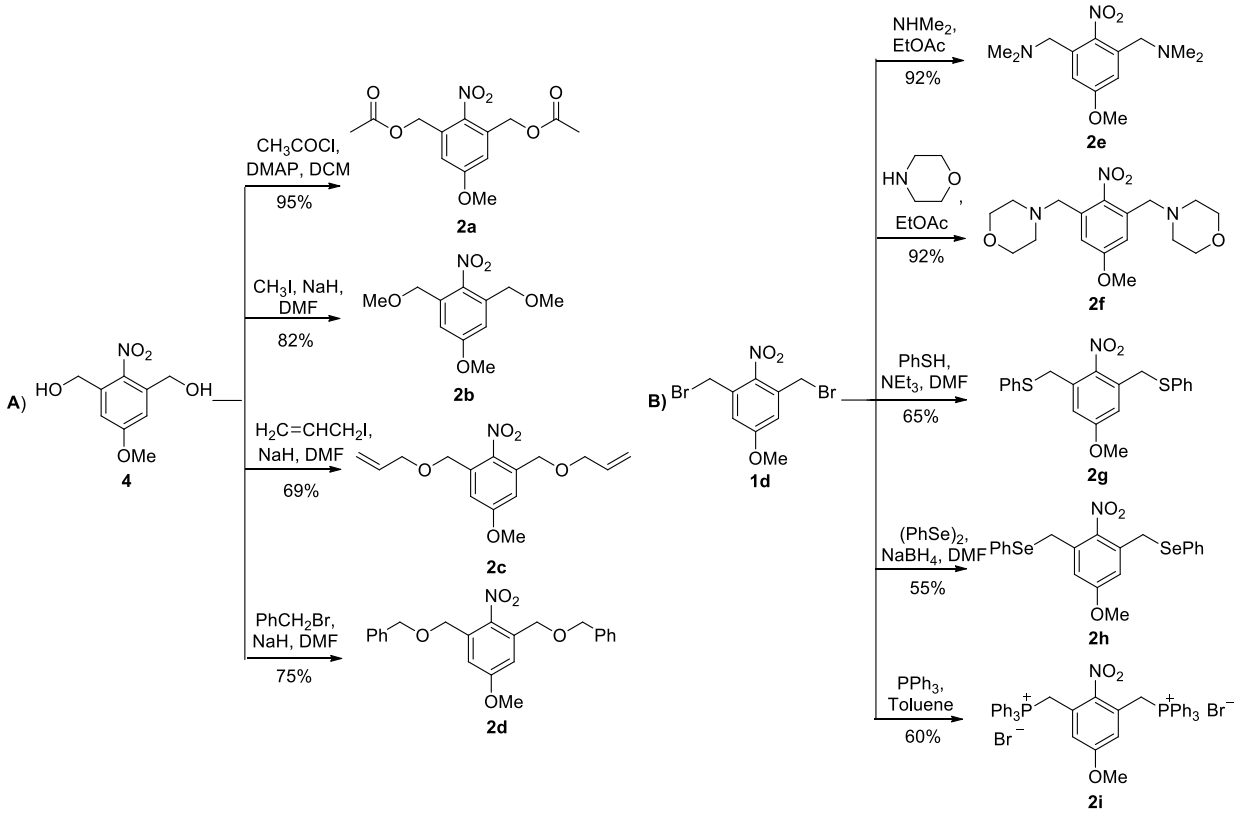

5'-dGCCTAGTTCTTTTAATTACTTGCAATGCAAGTAATTAAAGCTTGATCTG (**8a**)
3'-dCGGATCAAGAAAATTAATGAACGTTACGTTCATTAATTTCGAACTAGAC (**8b**)
8

In addition to the aromatic substituents, the leaving groups also greatly affect the ICL reaction rate. For **3a−i** containing a 2-methoxy group, compounds with phenylthio (**3g**) or phenyl selenide (**3h**) as leaving groups showed the fastest reaction rate. The moderate DNA cross-linking reaction rates were observed for those containing triphenylphosphonium (**3i**), methoxy (**3b**), or dimethylamine (**3e**) as leaving groups. The cross-linking reaction was greatly slowed down for compounds containing other leaving groups, including benzyloxy (**3d**), morpholine (**3f**), acetate (**3a**), or allyoxy group (**3c**). Among them, **3c** showed the slowest reaction rate. A slightly different trend for the reaction rates was observed for **2a−i** with a 2-NO_2 group (**2e** ≅ **2g** > **2i** > **2f** > **2h** > **2b** ≅ **2c** ≅ **2d** > **2a**). However, similar to 2-methoxy compounds, **2g** with phenylthio as a leaving group showed a relatively fast reaction rate for photoinduced DNA ICL formation. Compounds **2a−d** containing acetate or ether as leaving groups greatly slowed down photoinduced DNA cross-linking.

As the concentration of the substrates greatly affect the ICL efficiency,[4,16] we determined the optimized concentration (C_{opt}) for **2a−i** and **3a−i**. C_{opt} is defined as the minimum compound concentration required to obtain the possible highest ICL yields. The concentration-dependent DNA cross-linking study was performed with the optimized reaction time for **2a−i** and **3a−i** (Table 1 and Figures S19−S36, Supporting Information). Generally, the DNA ICL yields gradually improved with the increase of compounds' concentration. The DNA ICL reaction reached a balance for all compounds at the C_{opt} where the DNA alkylation reaction was completed and the highest DNA cross-linking efficiency was obtained. The C_{opt} was affected by both leaving groups and the aromatic substituents. The C_{opt} for compounds containing a 2-NO_2 group (**2a−i**) is in the order of **2h** (0.3 mM) < **2a−c** and **2i** (0.4 mM) < **2f** and **2g** (0.6 mM) < **2d** (0.8 mM) < **2e** (1.0 mM), while those containing a 2-OMe group showed a different C_{opt} order: **3i** (0.2 mM) < **3e** and **3f** (0.4 mM) < **3a** and **3d** (0.5 mM) < **3b**, **3g**, and **3h** (0.6 mM) < **3c** (2.0 mM). As the concentration of ODNs are constant for all tested compounds, a lower C_{opt} to reach the ICL reaction balance suggested a higher efficiency for generation of the carbocations that directly alkylated DNA. Among all compounds tested, **3i** with triphenylphosphonium as a leaving group showed a lowest C_{opt} that resulted in a relatively high ICL yield (34%). Compound **3d** with a benzyloxy group showed the highest ICL efficiency (37%) with a C_{opt} of 0.5 mM. Compound **3b** with methoxy as a leaving group showed a C_{opt} of 0.6 mM with a good ICL yield (34%). However, **3c** with an allyoxy leaving group showed the highest C_{opt} (2.0 mM) that may indicate a low efficiency for photogeneration of benzyl cations. Thus, triphenylphosphonium, benzyloxy, and methoxy groups may be considered good leaving groups for photogeneration of benzyl cations for this category of compounds.

Among **2a−i** and **3a−i**, compounds with a 2-methoxy group showed a higher ICL yield than the corresponding analogue having a 2-NO_2 group (**2a** vs **3a**, **2b** vs **3b**, etc.). This is well correlated with the electron-deficient nature of the carbocation intermediates that are stabilized by the presence of electron-donating groups. However, the effect of leaving groups on DNA cross-linking efficiency for 2-MeO compounds **3a−i** slightly differ from those of 2-nitro compounds **2a−i**. The ICL yields for **3a−i** under optimized conditions is in the order of **3d** > **3i** ≈ **3b** > **3a** ≈ **3c** ≈ **3g** > **3e** ≈ **3h** > **3f**, while 2-NO_2-

https://dx.doi.org/10.1021/acs.joc.0c02234
J. Org. Chem. XXXX, XXX, XXX−XXX

Scheme 3. Synthesis of 3a-i

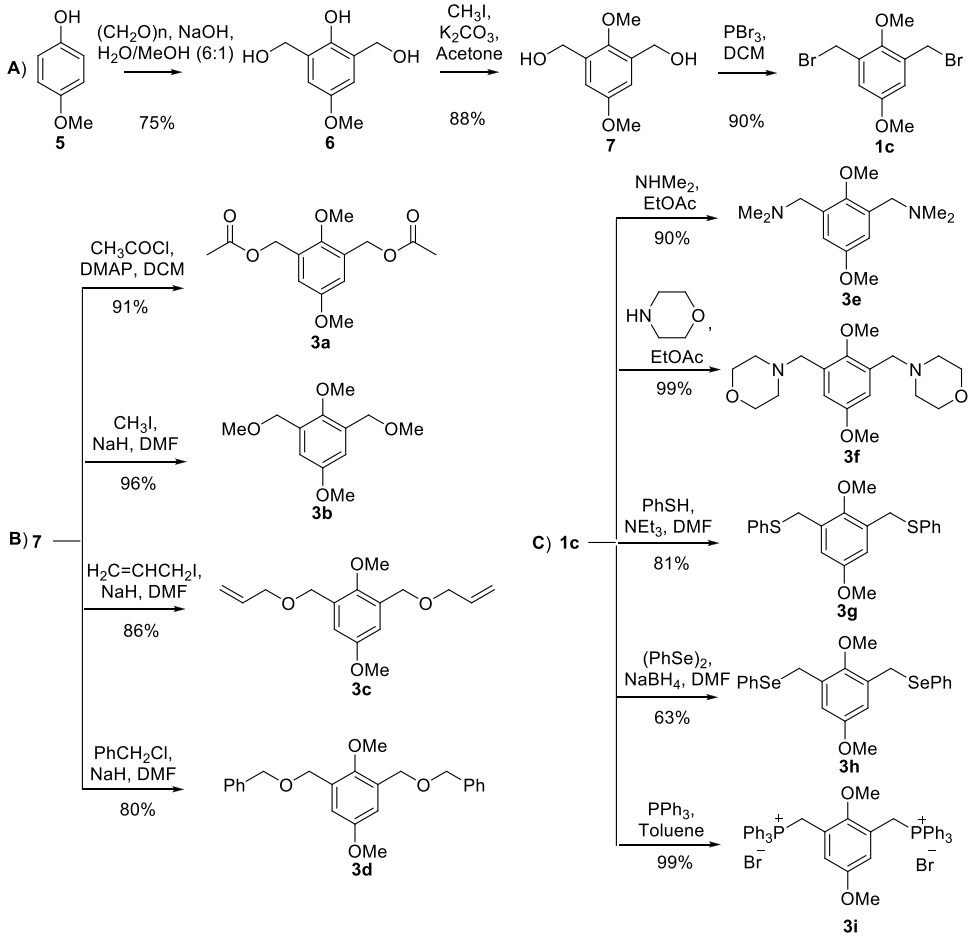

Table 1. Optimized Conditions, ICL Yields, and UV Absorption Data for 2a−i and 3a−i[a]

NO_2-Compd. (L)	RXN time (h)	con.[b] (mM)	ICL (%)[c]	λ_{max} (nm)	$\varepsilon_{\lambda max}$ ($L \cdot mol^{-1} \cdot cm^{-1}$)	OMe-Compd. (L)	RXN time (h)	con.[b] (mM)	ICL (%)[c]	λ_{max} (nm)	$\varepsilon_{\lambda max}$ ($L \cdot mol^{-1} \cdot cm^{-1}$)
2a (OAc)	44	0.4	18 ± 1	282, 347	4340, 2100	**3a** (OAc)	22	0.5	27 ± 3	286	2600
2b (OCH_3)	40	0.4	17 ± 2	282, 347,	3190, 1630	**3b** (OCH_3)	6	0.6	34 ± 3	286	2640
2c ($OCH_2CH{=}CH_2$)	40	0.4	14 ± 1	282, 347	3200, 1600	**3c** ($OCH_2CH{=}CH_2$)	36	2.0	28 ± 2	286	2900
2d (OCH_2Ph)	40	0.8	17 ± 2	282, 348	2920, 1400	**3d** (OCH_2Ph)	12	0.5	37 ± 1	287	3350
2e (NMe_2)	24	1	17 ± 2	273, 346	2760, 1040	**3e** (NMe_2)	6	0.4	25 ± 3	287	3120
2f [$N(CH_2CH_2)_2O$]	32	0.6	15 ± 1	273, 346	2640, 990	**3f** [$N(CH_2CH_2)_2O$]	12	0.4	18 ± 2	286	2940
2g (SPh)	24	0.6	23 ± 3	345	1750	**3g** (SPh)	2	0.6	28 ± 3	291	6900
2h (SePh)	36	0.3	21 ± 2	345	2190	**3h** (SePh)	2	0.6	24 ± 1	299	7050
2i (PPh_3)	28	0.4	21 ± 1	347	2030	**3i** (PPh_3)	5	0.2	34 ± 3	268, 302	7060, 5090

[a]The DNA cross-linking reaction was performed in a pH 8 phosphate buffer with 50 nM DNA duplex **8** upon 350 nm irradiation. [b]The minimum compound concentration needed to obtain the highest DNA cross-linking efficiency. [c]The maximum DNA ICL yield obtained for each compound under optimized conditions (all data are the average of three experiments).

containing compounds showed a different order (**2g** > **2h** ≈ **2i** > **2a** ≈ **2b** ≈ **2d** ≈ **2e** > **2f** ≈ **2c**). For 2-OMe-substituted compounds (**3a-i**), benzyloxy is the best leaving group for photoinduced DNA ICL formation while morpholine leads to the lowest cross-linking efficiency. For 2-nitro compounds, **2g** with a phenylthio group leads to the highest ICL yield while the allyloxy group showed the lowest ICL efficiency. Since different compounds showed a different C_{opt} value to obtain the highest DNA cross-linking efficiency, comparison of ICL yields obtained at the C_{opt} is not sufficient to conclude how the substituent and leaving group affect the ICL efficiency. For better comparison, the DNA cross-linking efficiency was

https://dx.doi.org/10.1021/acs.joc.0c02234
J. Org. Chem. XXXX, XXX, XXX−XXX

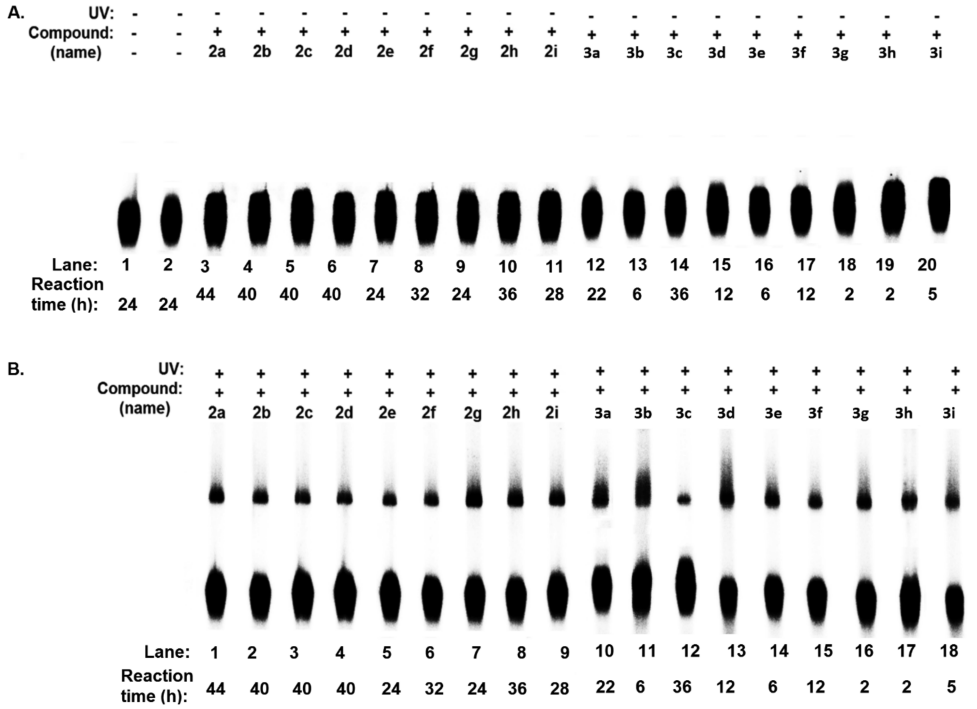

Figure 1. Photoinduced DNA ICL formation for **2a**−**i** and **3a**−**i**. (A) Lane 1: DNA only without UV irradiation; lane 2: DNA only with 350 nm irradiation for 24 h; lanes 3−20: DNA with **2a**−**i** or **3a**−**i** (500 μM) without UV irradiation; (B) lanes 1−18: DNA with **2a**−**i** or **3a**−**i** (500 μM) upon 350 nm irradiation for the designed time: lane 1: **2a** (ICL yield, 18 ± 2%). lane 2: **2b** (17 ± 2%); lane 3: **2c** (15 ± 1%) ; lane 4: **2d** (14 ± 2%); lane 5: **2e** (12 ± 1%); lane 6: **2f** (14 ± 2%); lane 7: **2g** (23 ± 3%); lane 8: **2h** (22 ± 2%); lane 9: **2i** (21 ± 3%); lane 10: **3a** (27 ± 2%); lane 11: **3b** (32 ± 4%) ; lane 12: **3c** (10 ± 1%); lane 13: **3d** (37% ± 3); lane 14: **3e** (26 ± 2%); lane 15: **3f** (18 ± 1%); lane 16: **3g** (26 ± 2%); lane 17: **3h** (21 ± 2%); lane 18: **3i** (34 ± 3%) (all ICL yields were obtained by triplicate experiments and shown as average ± standard deviation).

determined at the same concentration (500 μM) under the optimized reaction time for each compound (Figure 1). For both classes of compounds, the trend of ICL yields at 500 μM was similar to that obtained under the optimized conditions. Thus, we conclude that the electron-donating substituent increased the ICL efficiency while the electron-withdrawing substituent decreased the ICL efficiency. Both the leaving groups and the aromatic substituents combine to affect the efficiency of photoinduced DNA ICL formation.

Correlation between UV Absorbance and the Photoreactivity. Our previous results showed that the aromatic substituents greatly influenced the UV absorption of the compounds, which in turn affected the photoinduced DNA ICL formation.[4] In general, compounds with UV absorption closer to the irradiation wavelength (350 nm) and the stronger UV absorption led to a faster ICL reaction rate. In order to see the generality of this phenomenon, we investigated the influence of the leaving groups on the UV absorbance of **2a**−**i** and **3a**−**i**. UV/Vis spectra of these compounds were measured in CH_3CN with a 0.5 mM concentration (Figure S56, see the Supporting Information). The leaving groups slightly affected the UV absorption of these compounds, but there is no clear correlation between UV absorbance and the photoreactivity for these compounds (Table 1 and Figure S56). Although the highest photoreactivity of **3g** and **3h** seems to be well correlated with their UV absorbance [the longest maximum absorption wavelength (λ_{max}) and strongest absorption], such a correlation was not observed for others, such as **3a**−**e** and **2a**−**f**. For example, **3a**−**f** showed similar λ_{max} (~ 286−287 nm) with the absorbance order of **3d** > **3e** > **3c** ≈ **3f** > **3b** > **3a**, while their photoreactivity was observed in a different order (**3b** ≈ **3e** > **3d** ≈ **3f** > **3a** > **3c**). Similarly, **2a**−**d** showed similar λ_{max} (282 and 347 nm) with different absorbances. However, the absorbance order (**2a** > **2b** ≈ **2c** > **2d**) is opposite to that of the reactivity order (**2b** ≈ **2c** ≈ **2d** > **2a**). More interestingly, **2e** and **2f** showed a shorter λ_{max} and a weak absorption than **2a**−**d** but a much faster ICL reaction rate. Due to the complexity of DNA cross-linking reaction, the ICL efficiency could be affected by a variety of parameters, including the photosensitivity of the leaving groups, the UV absorption of the compounds, the efficiency for carbocation generation, the reactivity of carbocations (mono-alkylation and bisalkylation), and the competition of mono-alkylation and hydrolysis of carbocation with ICL formation. These compounds contain different leaving groups that would affect several of the above parameters, which could be one of the possible explanations for the inconsistency between their photoreactivity and UV absorption.

Mechanism of DNA ICL Formation and the Leaving Group Effects. Our previous study showed that the aromatic substituents greatly affected the mechanism for photoinduced DNA ICL formation via benzyl cations.[4,16] Two pathways were observed for cation generation from compounds containing trimethyl ammonium salts as the leaving groups upon 350 nm irradiation.[4,16] Compounds with electron-donating substituents (i.e., **1a**) generated the benzyl cations via oxidation of free radicals, while those with strong withdrawing groups (i.e., **1b**) underwent heterolytic cleavage of the C−N bond to generate benzyl cations (Scheme 1B,C). To further investigate the effect of leaving groups and aromatic substituents on DNA ICL formation, we performed free radical and carbocation trapping reactions with **2a**−**i** and **3a**−**i** that contain a wide variety of leaving groups. Methoxyamine and 2,2,6,6-tetramethylpiperidin-1-oxyl (TEMPO) were used as carbocation and radical

https://dx.doi.org/10.1021/acs.joc.0c02234
J. Org. Chem. XXXX, XXX, XXX−XXX

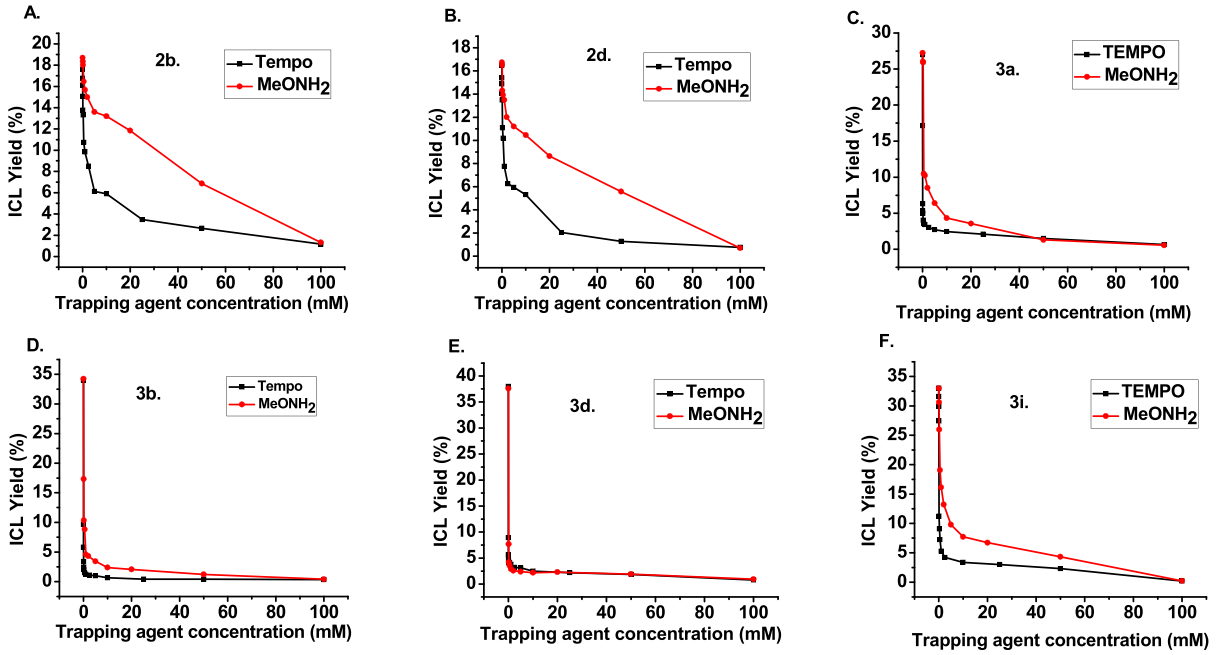

Figure 2. Carbocation and radical trapping with DNA ICL formation for **2b** (A), **2d** (B), **3a** (C), **3b** (D), **3d** (E), and **3i** (F).

Table 2. Cation and Radical Trapping Efficiency Evaluated from the Concentration of Methoxamine and TEMPO Required to Inhibit the ICL Yield to 5%, 2%, and Background Level[a]

NO_2-Compd. (L)	ICL[b] (%)	methoxyamine[c] (mM)			[TEMPO][d] (mM)			OMe-Comp. (L)	ICL[b](%)	methoxyamine[c] (mM)			[TEMPO][d] (mM)		
		5%	2%	B	5%	2%	B			5%	2%	B	5%	2%	B
2a (OAc)	16.2	35	70	100	5	22	50	**3a** (OAc)	27.1	10	40	40	0.1	25	50
2b (OCH_3)	18.2	68	92	100	15	70	100	**3b** (OCH_3)	34.1	1.0	20	20	0.05	0.25	10
2c ($OCH_2CH{=}CH_2$)	14.5	58	90	100	15	70	100	**3c** ($OCH_2CH{=}CH_2$)	26.3	2.0	20	20	0.025	1.0	25
2d (OCH_2Ph)	16.6	55	90	100	10	25	50	**3d** (OCH_2Ph)	37.8	0.2	10	10	0.05	25	25
2e (NMe_2)	17.6	15	35	50	25	70	100	**3e** (NMe_2)	25.7	2.0	10	10	1.5	2.5	10
2f [$N(CH_2CH_2)_2O$]	14.6	45	85	100	6	50	50	**3f** [$N(CH_2CH_2)_2O$]	18.8	3.0	30	30	3.0	15	25
2g (SPh)	23.4	35	50	50	10	70	100	**3g** (SPh)	28	1.5	5.0	5	1.0	1.5	2.5
2h (SePh)	22.2	75	95	100	15	65	100	**3h** (SePh)	24	1.0	5.0	5	0.05	0.25	2.5
2i (PPh_3)	20.8	60	90	100	30	90	100	**3i** (PPh_3)	33	40	80	80	1.0	55	100

[a]The DNA cross-linking reaction was performed in a pH 8 phosphate buffer with 50 nM DNA duplex **8** upon 350 nm irradiation. [b]The initial ICL yields without addition of methoxyamine or TEMPO. [c]The concentration of methoxamine required to inhibit ICL to 5% or 2%. [d]The concentration of TEMPO required to inhibit ICL to 5% or 2%.

traps, respectively (Figure 2 and Figures S37−S54). The ICL reactions were carried out under the optimized conditions for each compound in the presence of various concentrations of methoxyamine or TEMPO. The results for **2b**, **2d**, **3a**, **3b**, **3d**, and **3i** are shown in Figure 2, while the results for others are presented in Figures S37−S54. For all compounds tested, the ICL yields decreased with the addition of methoxyamine that acted as competitors for ICL formation. The DNA ICL formation was completely inhibited when the concentration of methoxyamine increased to a certain level, indicating that carbocations were involved in the DNA cross-linking process.

However, the trapping efficiency strongly depended on the substrates, which was measured as the minimal concentration of the trapping agents required to decrease the ICL yields to a similar level (5%, 2%, or the background level) (Table 2). In general, trapping of the benzyl cations generated from **3a−i** with an OMe group is much more efficient than those generated from the corresponding NO_2-containing compounds **2a−i**. For example, 0.2 mM methoxamine decreased the ICL yield of **3d** from 37.8% to 5% while ∼55 mM methoxyamine was required to inhibit DNA ICL formation of **2d** from 16.6% to 5% (Figure 2B,E and Table 2). Similarly, the concentration of methoxyamine for inhibition of ICL formation to 5% is 68 mM for **2b** and 75 mM for **2h** that is about 70 times higher than that needed for **3b** and **3h** (∼1.0 mM) (Figure 2A,D and Table 2). A similar phenomenon was observed for other compounds (Table 2, **2a** vs **3a**, **2c** vs **3c**, **2e−g** vs **3e−g**, and **2i** vs **3i**). Higher cation trapping efficiency for **3a−i** than **2a−i** suggested higher reactivity of the benzyl cations photogenerated from **3a−i** than those produced from **2a−i**. Similarly, to decrease the ICL yields to 2%, much higher concentrations of methoxyamine were needed for **2a−i** than those for **3a−i**. This is well correlated with the electron-deficient property of the carbocations that were stabilized by electron-donating groups leading to higher reactivity. Among compounds **3a−i** that contain the same aromatic substituent

https://dx.doi.org/10.1021/acs.joc.0c02234
J. Org. Chem. XXXX, XXX, XXX−XXX

Scheme 4. Proposed Mechanism for DNA ICL Formation Induced by 2a−i and 3a−i

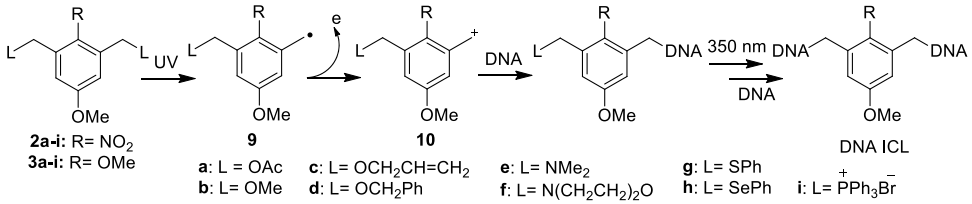

(2,4-dimethoxy groups), the leaving groups also affected the cation-trapping efficiency. The highest concentration of methoxyamine was needed for inhibiting ICL formation induced by **3i** having triphenylphosphonium salt as a leaving group, which might be due to the strong withdrawing property of the triphenylphosphonium salt (Figure 2F and Table 2). Similarly, **3a** with a withdrawing acetate group showed a lower cation-trapping efficiency than **3b−h** (Figure 2C and Table 2).

Considering that the benzyl cations can be generated either from oxidation of the corresponding free radicals (**pathway 1**) or by direct heterolysis of C−X bonds (**pathway 2**), we performed free radical trapping experiments using excess TEMPO. Similar to cation trapping, the addition of TEMPO suppressed the DNA ICL formation for all compounds (**2a−i** and **3a−i**) tested. The ICL yields gradually decreased to the background level with increased concentration of TEMPO (Figure 2 and Figures S37−S54). These results suggested that the free radicals were involved in the DNA ICL formation process. However, the trapping efficiency strongly depended on the substrates. Trapping of the free radicals generated from **3a−i** with an OMe substituent was more efficient than those generated from the corresponding NO_2-containing compounds **2a−i**. For example, 0.05 mM TEMPO decreased the ICL yield of **3d** from 37.8% to 5% while it required ∼10 mM TEMPO to obtain a similar trapping efficiency for **2d** (from 16.6% to 5%) (Figure 2B,E and Table 2). Similarly, much higher concentrations of TEMPO were needed for **2a−c** and **2e−i** than the corresponding **3a−c** and **3e−i** to reach the same trapping efficiency (Table 2). This is well correlated with the electron-deficient property of the free radicals that were stabilized by electron-donating groups leading to higher reactivity. Collectively, the results of cation trapping and free radical trapping study suggested that the benzyl cations were generated through oxidation of the free radicals (**pathway 1**, Scheme 1B). Thus, we propose that photoirradiation of **2a−i** and **3a−i** generated the free radicals (**9**) that were further converted to the benzyl cations (**10**) that alkylated DNA (Scheme 4).

In order to provide direct evidence for the formation of benzyl radicals and benzyl carbocations, we performed monomer trapping reaction to isolate cation or free radical trapping adducts. Compound **3i** was selected as a representative for monomer trapping reactions because it is relatively easy to synthesize and showed a relatively high ICL yield and fast reaction rate. The trapping reactions were performed with **3i** in the presence of excess methoxyamine or TEMPO that served as carbocation and free radical traps, respectively. Thin-layer chromatography (TLC) indicated a very complex reaction for the cation trapping. Several new spots with similar R_f values were observed, which were not separable by chromatography. Thus, LC-MS was used for the analysis of the adducts formed in the monomer trapping reaction (Figure S57). The LC-MS analysis revealed two major peaks eluting at ∼57.8 and ∼60.4 min for *m*/*z* 461 (**11a**) and 470 (**11b**) (Scheme 5 and Supporting Information, Figure S57A−C, LC-mass data)

Scheme 5. Cation and Free Radical Trapping Products Obtained with 3i upon 350 nm Irradiation

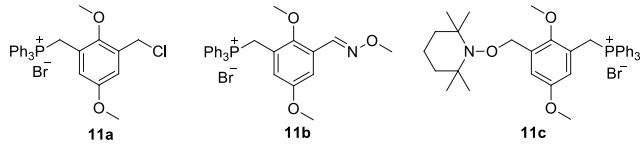

11a
Calcd. $(M-Br)^+$: 461.1432
Found $(M-Br)^+$: 461.1408

11b
Calcd. $(M-Br)^+$: 470.1880
Found $(M-Br)^+$: 470.1839

11c
Calcd. $(M-Br)^+$: 582.3132
Found $(M-Br)^+$: 582.3115

(Note: $MeONH_2$·HCl was used for cation trapping, which is the source of the chloro group in **11a**). The mass of two adducts **11a** and **11b** was further confirmed by HRMS (Scheme 5 and Supporting Information, Figure S57E,F, HRMS data). Formation of the adducts **11a** and **11b** suggested that the mono carbocation (**10**) was generated upon photoirradiation of **3i**. The free radical trapping reaction provided one major product **11c** that was isolated by chromatography. The structure of **11c** was determined by NMR and HRMS, suggesting the formation of mono radical (**9**). Generation of mono-trapping products **11a−c** provided direct evidence for our proposed mechanism. Departure of two leaving groups occurred in a stepwise manner, leading to the formation of mono-radical **9** and mono-cation **10**. Failure to detect the biscation-trapping products even with a longer period of photoirradiation indicated a much lower efficiency for photoactivation of the second leaving group that should be the rate-determining step for ICL formation.

Determination of DNA Alkylation Sites and the Effect of the Aromatic Substituents and Leaving Groups. It was well known that the N7-alkylated purines can be cleaved upon heating in the presence of piperidine.[48−50] Previously, we have determined the alkylation sites of photogenerated benzyl cations by studying the heat stability of the cross-linked DNA and/or synthesizing the adducts formed between benzyl cations and natural nucleosides.[4] Although the monomer reaction showed that the photogenerated benzyl cations could react with dC, dA, and dG, the heat stability study of the cross-linked DNA indicated that dGs were preferred alkylation sites in ODNs. In order to investigate the effect of leaving groups and the aromatic substituents on the alkylation sites of **2a−i** and **3a−i**, we performed the heat stability study with ICL products formed with these compounds. We isolated both single-stranded ODNs (p^{32}-ODN **8a′**) as well as the ICL products formed with DNA duplex **8** upon 350 nm irradiation in the presence of **2a−i** and **3a−i**. The heat stability data of the isolated p^{32}-ODN **8a′** and the ICL products for **3a** and **2a** are shown in Figure 3, while the data for other compounds are shown in Figure S55. Similar to a previous study, the ICL products were relatively stable upon heating in a pH 7.0

https://dx.doi.org/10.1021/acs.joc.0c02234
J. Org. Chem. XXXX, XXX, XXX−XXX

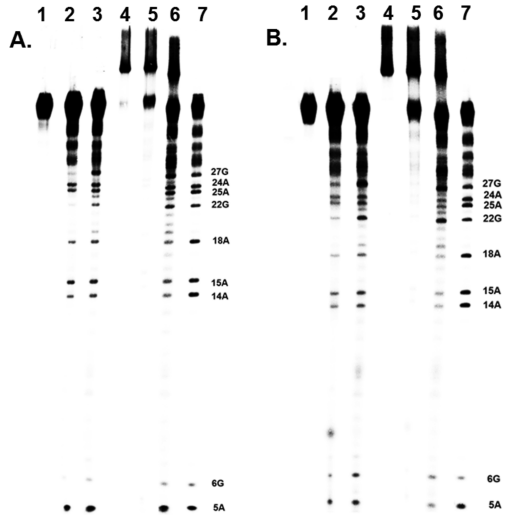

Figure 3. Determination of the reaction sites of **3a** (A) and **2a** (B). Phosphorimage autoradiogram of 20% denaturing PAGE analysis of the isolated DNA ICL products and alkylated single-stranded DNA (**8a′**) upon heating in piperidine or phosphate buffer. The ICL product and **8a′** were produced by 350 nm irradiation of duplex **8** in the presence of **3a** (500 μM) or **2a** (400 μM). **8a** was radiolabeled at the 5′-terminus. Lane 1: isolated alkylated single-stranded DNA (**8a′**). Lane 2: **8a′** was heated in a pH 7 phosphate buffer at 90 °C for 30 min. Lane 3: **8a′** was heated in 1.0 M piperidine at 90 °C for 30 min. Lane 4: isolated DNA ICL products. Lane 5: the DNA ICL products were heated in a pH 7 phosphate buffer at 90 °C for 30 min. Lane 6: the DNA ICL products were heated in 1.0 M piperidine at 90 °C for 30 min. Lane 7: G+A sequencing.

phosphate buffer for 30 min, while obvious cleavage bands were observed upon heating in 1.0 M piperidine. For most compounds tested (i.e., **2a−i**, **3c**, and **3e−i**), the cleavage mainly occurred at dG sites and to a lesser extent at dAs (Figure 3B and Figure S55). However, **3a**, **3b**, and **3d** showed the major cleavage sites not only at dGs but also at dAs, which is different from a previous observation (Figure 3A and Figure S55). These data suggested that both substituents and leaving groups affected the reactivity of these photogenerated benzyl cations toward DNA. For comparison of the relative reactivity of these benzyl cations toward dG and dA, we estimated the percentages for cleavages at dG_{27}, G_{22}, dA_{25}, and dA_{24} sites. From the cleavage ratio of dG_{27}+dG_{22} to dA_{25}+dA_{24} ($Cleav_{dG/dA}$), we are able to estimate the relative photoreactivity of these compounds toward dG and dA in ODNs (Table 3). Compounds **2a−i**, **3c**, and **3e−i** showed a $Cleav_{dG/dA}$ of ∼2 or higher, indicating that dGs were the preferred alkylation sites for the benzyl cations produced from these compounds. However, **3a**, **3b**, and **3d** showed a much smaller $Cleav_{dG/dA}$ ($Cleav_{dG/dA}$ ≈ 1) than **2a**, **2b**, and **2d** ($Cleav_{dG/dA}$ = 1.6−2.6), which suggested that **3a**, **3b**, and **3d** had improved reactivity toward dAs. It is well known that an electron-donating aromatic substituent increases the stability of benzyl-like carbocations.[51] Thus, the methoxy-substituted benzyl carbocations generated from **3a**, **3b**, and **3d** are expected to be more stable than the corresponding nitro-substituted benzyl carbocations generated from **2a**, **2b**, and **2d**, which in turn lead to increased reactivity of **3a**, **3b**, and **3d** toward dA.

From the heat stability study, we were able to conclude that **2a−i** and **3a−i** alkylated dG and/or dA sites upon 350 nm irradiation but different compounds showed a slightly different

Table 3. Photoreactivity of 2a−i and 3a−i toward dG and dA Evaluated from the Ratio for Cleavage at dG_{27}, dG_{22}, dA_{25}, and dA_{24}[a]

NO_2-Compd. (L)	cleav.[b] (dG/dA)	OMe-Compd. (L)	cleav.[b] (dG/dA)
2a (OAc)	1.63	**3a** (OAc)	0.98
2b (OCH_3)	2.86	**3b** (OCH_3)	1.19
2c ($OCH_2CH{=}CH_2$)	2.19	**3c** ($OCH_2CH{=}CH_2$)	1.83
2d (OCH_2Ph)	2.59	**3d** (OCH_2Ph)	1.07
2e (NMe_2)	2.20	**3e** (NMe_2)	2.02
2f [$N(CH_2CH_2)_2O$]	2.12	**3f** [$N(CH_2CH_2)_2O$]	2.16
2g (SPh)	2.69	**3g** (SPh)	1.82
2h (SePh)	2.01	**3h** (SePh)	1.69
2i (PPh_3)	2.08	**3i** (PPh_3)	2.73

[a]The DNA cross-linking reaction was performed in a pH 8 phosphate buffer with 50 nM DNA duplex **8** upon 350 nm irradiation. The ICL products were isolated and heated in 1.0 M piperidine at 90 °C for 30 min. The cleavage bands at dG_{27}, dG_{22}, dA_{25}, and dA_{24} were quantified. [b]The ratio of cleavage at dG_{27}+dG_{22} to that at dA_{25}+dA_{24}.

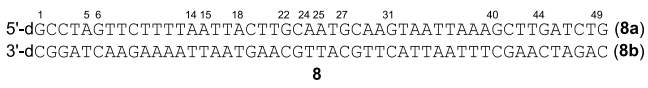

reactivity toward dG and dA. To investigate whether the alkylation could occur with pyrimidines, we tested the ICL reaction with duplex **12** containing dCs/dTs in one strand and dGs/dAs in the complimentary strand (Figure 4A). ICL formation was observed when duplex **12** was treated with **3d** (6.4%), **3i** (5.1%), **2g** (6.4%), and **2i** (7.7%), which suggested that dC and/or dT are possible alkylation sites (Figure 4A). To further investigate the cross-linking sites, we synthesized one self-complementary dAT sequences (**13**) that was treated with **3d**, **3i**, **2g**, and **2i** upon 350 nm irradiation. The DNA ICL formation was not observed with **13**, indicating that interstrand cross-linking reaction did not take place between dA and opposing dT neither with staggered dA/dA (Figure 4B). However, the cleavage bands were observed with dAs when the single-stranded ODN **13a′** was isolated from the cross-linking reaction mixture and heated in 1.0 M piperidine at 90 °C for 30 min (Figure 4C). This suggested that mono-alkylation occurred with dAs. Collectively, these data indicated that ICL reactions took place with opposing dG/dC but not with dA/dT or staggered dA/dA while mono-alkylation could take place with dAs.

■ CONCLUSIONS

We have demonstrated that two series of benzene analogues containing a wide variety of leaving groups are photoactivatable bisalkylating agents. These compounds efficiently induced DNA ICL formation upon 350 nm irradiation via benzyl cations that were formed from the oxidation of the photogenerated benzyl radicals. Determination of cation and free radical trapping adducts provided direct evidence for the formation of benzyl radicals and carbocations. Compounds with an electron-donating group (OMe) (**3a−i**) showed a higher cross-linking efficiency and faster reaction rate than the corresponding ones having withdrawing group (NO_2) (**2a−i**) regardless of which leaving group is present. Benzylic leaving groups also have big effects on DNA ICL efficiency. Among all OMe-containing compounds, **3b** (L = OMe), **3d** (L = OCH_2Ph), and **3i** (L = PPh_3^+) are the most efficient

https://dx.doi.org/10.1021/acs.joc.0c02234
J. Org. Chem. XXXX, XXX, XXX−XXX

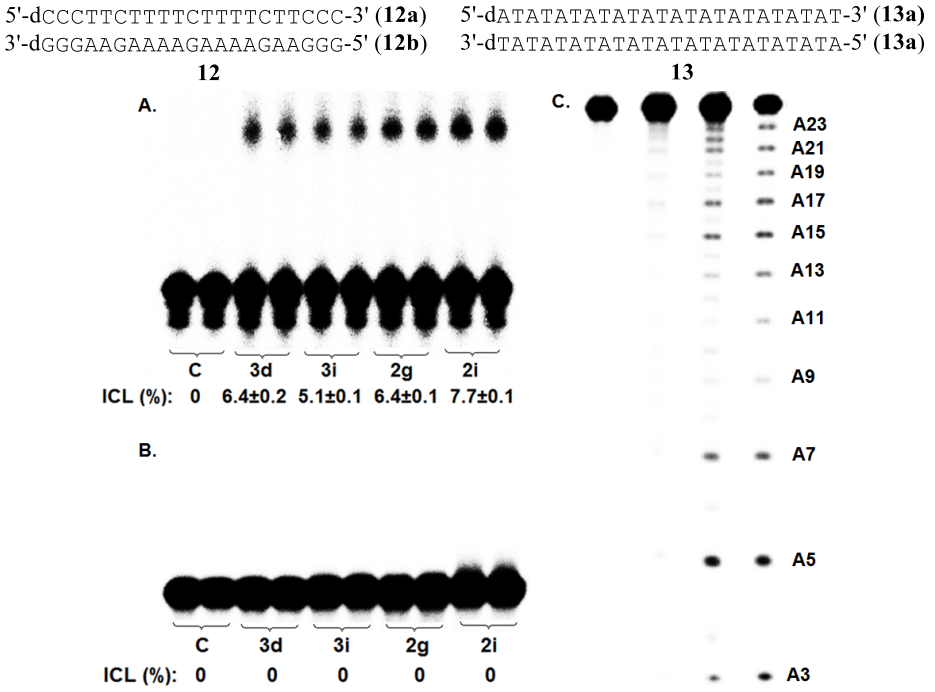

Figure 4. Photoinduced DNA ICL formation for **3d**, **3i**, **2g**, and **2i** with duplex **12** (**A**) and duplex **13** (B) and determination of the reaction sites of **3i** in duplex **13** (**C**) [phosphorimage autoradiogram of 20% denaturing PAGE analysis of the ICL reaction mixture upon heating in piperidine or phosphate buffer. An ICL reaction mixture of **13** (50 nM) and **3i** (0.2 mM) in pH 8 phosphate buffer was irradiated with 350 nm for 5 h. The single-stranded ODN (5′-p^{32}-**13a**′) was isolated from the cross-link reaction mixture. Lane 1: the isolated single-stranded ODN (**13a**′); Lane 2: **13a**′ was heated in a pH 7 phosphate buffer at 90 °C for 30 min; Lane 3: **13a**′ was heated in 1.0 M piperidine at 90 °C for 30 min; Lane 4: G+A sequencing].

photoactivated DNA cross-linkers with an ICL yield of >34%, while **3f** with morpholine as a leaving group resulted in the lowest ICL yield (18%). Although the benzyl cations photogenerated from these compounds alkylated dG, dA, and dC, the ICL formation only took place with opposing dG/dC not with staggered dA/dA. Both aromatic substituents and leaving groups strongly affected the photoreactivity of these compounds toward dG and dA. Compounds **2a**–**i**, **3c**, and **3e**–**i** showed better photoreactivity toward dG than dA, while **3a** (L = OAc), **3b** (L = OMe), and **3d** (L = OCH_2Ph) showed a similar reactivity toward dGs and dAs. This systematic study provides valuable fundamentals for developing more efficient photoinduced DNA cross-linking agents. It also provides guidelines for development of photoactivated drugs.

EXPERIMENTAL SECTION

General Experimental Methods. All reactions were stirred magnetically, unless otherwise noted. An oil bath was used as a heating source for all of the organic synthesis reactions that required heating in this work. A heating block or water bath were used for DNA reactions involving heating. Reactions were monitored by thin-layer chromatography (TLC): Merck Silica Gel 60 F254. All chemicals came from commercially available source without further purification. Oligonucleotides were synthesized via standard automated DNA synthesis techniques. Deprotection of the synthesized DNA were performed with a mixture of 40% aqueous $MeNH_2$ and 28% aqueous NH_3 (1:1) at room temperature for 2 h. 20% Denaturing polyacrylamide gel electrophoresis was used for DNA purification. [γ-^{32}P] ATP was used for DNA labeling with a standard method. Quantification of radiolabeled oligonucleotides was carried out using a Molecular Dynamics phosphorimager equipped with ImageQuant, version 5.2, software. For all phosphorimage autoradiograms, the top dark spot that migrated slowest is considered as the DNA cross-link product and the bottom dark spot is considered as the single-stranded ODN, which were determined using a molecular ladder.[24] A UV experiment was carried out using an RPR-100 Photochemical Reactor with RPR-3500 Å. ^{1}H NMR and 13C{1H} NMR spectra were taken on either a Bruker DRX 300 or DRX 500 MHz spectrophotometer with TMS as an internal standard. High-resolution mass spectrometry IT-TOF was used for molecular measurement.

*(5-Methoxy-2-nitro-1,3-phenylene)bis(methylene) Diacetate (**2a**).* Compound **4** (300 mg, 1.41 mmol) and 4-dimethyl aminopyridine (517 mg, 4.23 mmol) in DCM was cooled to 0 °C. Acetyl chloride (443 mg, 5.64 mmol) was added using a syringe. The reaction mixture was warmed to rt, stirred overnight, quenched with H_2O (10 mL), and extracted with DCM (3 × 15 mL). The combined organic layers were washed with brine, dried over anhydrous Na_2SO_4, and concentrated. The remaining residue was purified by column chromatography (Hexane:Ethyl acetate = 2:1, R_f = 0.35) to obtain **2a** as a light yellow solid (397 mg, 95%), m.p. 95–96 °C. ^{1}H NMR (300 MHz, $CDCl_3$): δ 6.96 (s, 2H), 5.23 (s, 4H), 3.89 (s, 3H), 2.11 (s, 6H). 13C{1H} NMR (75 MHz, $CDCl_3$): δ 170.2, 161.2, 141.7, 132.8, 114.2, 62.4, 55.9, 20.6. HRMS-ESI (+) (m/z): $[M + Na]^+$ calcd. for $C_{13}H_{15}NO_7Na^+$, 320.0741; found: 320.0737.

*5-Methoxy-1,3-bis(methoxymethyl)-2-nitrobenzene (**2b**).* NaH (169 mg, 60%, 4.23 mmol) was added to a solution of **4** (300 mg, 1.41 mmol) in DMF (6.0 mL) at 0 °C. The reaction mixture was stirred for 10 min at 0 °C. Then, CH_3I (800 mg, 5.64 mmol) was added. The reaction mixture was allowed to warm to rt, stirred overnight, quenched with water (10 mL), and extracted with ethyl acetate (3 × 15 mL). The organic layers were combined, washed with brine, dried over anhydrous Na_2SO_4, and concentrated. The remaining residue was purified by column chromatography (Hexane:Ethyl acetate = 2:1, R_f = 0.68) to obtain **2b** as a yellow solid (280 mg, 82%), m.p. 39–40 °C. ^{1}H NMR (300 MHz, $CDCl_3$): δ 7.05 (s, 2H), 4.58 (s, 4H), 3.90 (s, 3H), 3.43 (s, 6H). 13C{1H} NMR (75 MHz, $CDCl_3$): δ 161.5, 140.9, 135.3, 112.6, 71.7, 58.8, 55.8. HRMS-ESI (+) (m/z): $[M - OMe]^+$ calcd. for $C_{10}H_{12}NO_4^+$, 210.0761; found: 210.0755.

https://dx.doi.org/10.1021/acs.joc.0c02234
J. Org. Chem. XXXX, XXX, XXX–XXX

*1,3-Bis((allyloxy)methyl)-5-methoxy-2-nitrobenzene (**2c**).* NaH (169 mg, 60%, 4.23 mmol) was added to a solution of **4** (300 mg, 1.41 mmol) in DMF (6.0 mL) at 0 °C. The resulting mixture was stirred for 10 min. Then, allyl iodide (948 mg, 5.64 mmol) was added. The reaction mixture was allowed to warm to rt, stirred overnight, quenched with water (10 mL), and extracted with ethyl acetate (3 × 15 mL). The organic layers were combined, washed with brine, dried over anhydrous Na_2SO_4, and concentrated. The remaining residue was purified by column chromatography (Hexane:Ethyl acetate = 2:1, R_f = 0.8) to obtain **2c** as a yellowish liquid (286 mg, 69%). ^{1}H NMR (300 MHz, $CDCl_3$): δ 7.09 (s, 2H), 6.00−5.88 (m, 2H), 5.35 (s, 1H), 5.30 (s, 1H), 5.25−5.22 (d, J = 9.0 Hz, 2H), 4.64 (s, 4H), 4.07−4.05 (d, J = 6.0 Hz, 4H), 3.89 (s, 3H). 13C{1H} NMR (75 MHz, $CDCl_3$): δ 161.5, 141.0, 135.4, 134.0, 117.6, 112.7, 71.9, 68.2, 55.8. HRMS-ESI (+) (m/z): $[M - OC_3H_5]^+$ calcd. for $C_{12}H_{14}NO_4^+$, 236.0917; found: 236.0915.

*((((5-Methoxy-2-nitro-1,3-phenylene)bis(methylene))bis(oxy))-bis(methylene))dibenzene (**2d**).* A solution of **4** (300 mg, 1.41 mmol) in DMF (6.0 mL) was cooled to 0 °C followed by the addition of NaH (169 mg, 60%, 4.23 mmol). The resulting mixture was stirred for 10 min. Then, benzyl bromide (720 mg, 4.23 mmol) was added. The reaction mixture was allowed to warm to rt, stirred overnight, quenched with water (10 mL), and extracted with ethyl acetate (3 × 15 mL). The organic layers were combined, washed with brine, dried over anhydrous Na_2SO_4, and concentrated. The residue was purified by column chromatography (Hexane:Ethyl acetate = 2:1, R_f = 0.76) to afford **2d** as a yellow oily (414 mg, 75%). ^{1}H NMR (300 MHz, $CDCl_3$): δ 7.42−7.30 (m, 10H), 7.12 (s, 2H), 4.71 (s, 4H), 4.60 (s, 4H), 3.88 (s, 3H). 13C{1H} NMR (75 MHz, $CDCl_3$): δ 161.5, 141.2, 137.6, 135.3, 128.5, 127.9, 127.8, 112.9, 73.2, 68.5, 55.8. HRMS-ESI (+) (m/z): $[M + Na]^+$ calcd. for $C_{23}H_{23}NO_5Na^+$, 416.1468; found: 416.1453.

*1,1′-(5-Methoxy-2-nitro-1,3-phenylene)bis(N,N-dimethylmethanamine) (**2e**).* Into a solution of **1d** (150 mg, 0.44 mmol) in ethyl acetate (4.0 mL) was added dimethylamine solution (2.0 M in methanol) (2.2 mL, 4.4 mmol). The reaction mixture was stirred at rt for 8 h and concentrated. The residue was purified by column chromatography (DCM:Methanol = 10:1, R_f = 0.5) to afford **2e** as a yellowish solid (108 mg, 92%), m.p. 44−45 °C. ^{1}H NMR (300 MHz, $CDCl_3$): δ 7.05 (s, 2H), 3.89 (s, 3H), 3.51 (s, 4H), 2.26 (s, 12H). 13C{1H} NMR (75 MHz, $CDCl_3$): δ 160.5, 144.2, 133.3, 114.6, 59.6, 55.9, 45.2. HRMS-ESI (+) (m/z): $[M + H]^+$ calcd. for $C_{13}H_{22}N_3O_3^+$, 268.1656; found: 268.1633.

*4,4′-((5-Methoxy-2-nitro-1,3-phenylene)bis(methylene))-dimorpholine (**2f**).* Morpholine (387 mg, 4.40 mmol) was added to a solution of **1d** (150 mg, 0.44 mmol) in ethyl acetate (2 mL). The resulting mixture was stirred at rt overnight and concentrated. The residue was purified by column chromatography (DCM:Methanol = 10:1, R_f = 0.72) to afford **2f** as a yellowish solid (143 mg, 92%), m.p. 88−89 °C. ^{1}H NMR (300 MHz, $CDCl_3$): δ 6.89 (s, 2H), 3.88 (s, 4H), 3.66 (s, 8H), 3.57 (s, 3H), 2.41 (s, 8H). 13C{1H} NMR (75 MHz, $CDCl_3$): δ 160.2, 144.3, 133.7, 114.5, 66.8, 59.3, 55.8, 53.3. HRMS-ESI (+) (m/z): $[M + H]^+$ calcd. for $C_{17}H_{26}N_3O_5^+$, 352.1867; found: 352.1865.

*((5-Methoxy-2-nitro-1,3-phenylene)bis(methylene))Bis-(phenylsulfane) (**2g**).* Into a solution of **1d** (170 mg, 0.5 mmol) in DMF (5.0 mL) was added thiophenol (165.3 mg, 1.5 mmol) followed by trimethylamine (0.6 mL). The reaction mixture was stirred at 70 °C overnight, quenched with water (10 mL), and extracted with ethyl acetate (3 × 15 mL). The organic layers were combined, washed with brine, dried over anhydrous Na_2SO_4, and concentrated. The residue was purified by column chromatography (Hexane:ethyl acetate = 5:1, R_f = 0.45) to afford **2g** as a yellowish solid (130 mg, 65%), m.p. 73−74 °C. ^{1}H NMR (300 MHz, $CDCl_3$): δ 7.30−7.26 (m, 10H), 6.65 (m, 2H), 4.15 (s, 4H), 3.64 (s, 3H). 13C{1H} NMR (75 MHz, $CDCl_3$): δ 160.1, 143.4, 134.7, 133.5, 131.4, 129.0, 127.4, 114.9, 55.6, 36.1. HRMS-ESI (+) (m/z): $[M + K]^+$ calcd. for $C_{21}H_{19}NO_3S_2K^+$, 436.0438; found: 436.0429.

*((5-Methoxy-2-nitro-1,3-phenylene)bis(methylene))bis-(phenylselane) (**2h**).* Into a solution of diphenyl diselenide (368.3 mg, 1.18 mmol) in DMF (5.0 mL) was added $NaBH_4$ (11.2 mg, 0.295 mmol). The reaction mixture was stirred at rt for 2 h. Then, a solution of **1d** (100 mg, 0.295 mmol) in DMF (2.0 mL) was added. The resulting mixture was stirred at rt for another 4 h, quenched with water (10 mL), extracted with ethyl acetate (3 × 15 mL). The organic layers were combined, washed with brine, dried over anhydrous Na_2SO_4, and concentrated. The residue was purified by column chromatography (Hexane:ethyl acetate = 5:1, R_f = 0.4) to afford **2h** as a light yellow solid (80.0 mg, 55%): m.p. 95−97 °C. ^{1}H NMR (300 MHz, $CDCl_3$): δ 7.50−7.48 (d, J = 6.0 Hz, 4H), 7.30−7.27 (m, 6H), 6.32 (s, 2H), 4.08 (s, 4H), 3.53 (s, 3H). 13C{1H} NMR (75 MHz, $CDCl_3$): 159.5, 135.1, 134.7, 129.0, 128.9, 128.9, 127.8, 114.5, 55.1, 28.3. HRMS-ESI (+) (m/z): $[M + K]^+$ calcd. for $C_{21}H_{19}NO_3Se_2K^+$, 531.9331; found: 531.9320.

*((5-Methoxy-2-nitro-1,3-phenylene)bis(methylene))bis-(triphenylphosphonium) Bromide (**2i**).* A mixture of **1d** (170 mg, 0.5 mmol) and triphenylphosphine (289 mg, 1.1 mmol) in dry toluene (5 mL) was stirred at rt for 2 days under argon. The crude white powder was obtained by filtration, which was purified by column chromatography (DCM:Methanol = 10:1, R_f = 0.32) to afford **2i** as a yellowish foam (259 mg, 60%). ^{1}H NMR (300 MHz, $CDCl_3$): δ 7.83−7.78 (m, 6H), 7.71−7.55 (m, 24H), 7.18 (s, 2H), 5.58−5.53 (d, J = 15.0 Hz, 4H), 3.46 (s, 3H). 13C{1H} NMR (75 MHz, $CDCl_3$): δ 161.4, 143.1, 135.5, 134.3, 134.2, 130.6, 130.5, 126.9, 126.8, 120.2, 117.3, 116.2, 55.6, 30.9, 29.3, 28.6. HRMS-ESI (+) (m/z): $[M - 2Br]^{2+}$ calcd. for $C_{45}H_{39}NO_3P_2^{2+}$, 351.6197; found: 351.6183.

*(2-Hydroxy-5-methoxy-1,3-phenylene)dimethanol (**6**).* A solution of **5** (50 g, 0.4 mol) in H_2O (180 mL) was added NaOH (16 g, 0.4 mol) and stirred till obtaining a clear solution. Then, paraformaldehyde (18.0 g, 0.6 mol) and methanol (30 mL) were added. The reaction mixture was stirred at 30 °C for 2 days and acidified with HCl (5.0 M) to pH 5.0. Then, methanol was removed. The resulting aqueous solution was extracted with ethyl acetate (3 × 100 mL). The organic layers were combined, washed with brine, dried over anhydrous Na_2SO_4, and concentrated. The residue was purified by column chromatography (Hexane:Ethyl acetate = 1:1, R_f = 0.33) to obtain **6** as a white solid (55.2 g, 75%). ^{1}H NMR (300 MHz, DMSO-d_6): δ 8.04 (s, 1H), 6.76 (s, 2H), 5.24−5.20 (t, J = 6.0 Hz, 2H), 4.54−4.52 (d, J = 6.0 Hz, 4H), 3.68 (s, 3H) (the NMR spectra were in agreement with those reported).[52]

*(2,5-Dimethoxy-1,3-phenylene)dimethanol (**7**).* A solution of **6** (18.4 g, 0.1 mol) in acetone (100 mL) was added K_2CO_3 and CH_3I. The reaction mixture was stirred at 50 °C overnight and concentrated. Then, water (50 mL) was added. The resulting aqueous solution was extracted with ethyl acetate (3 × 80 mL), washed with brine, dried over anhydrous Na_2SO_4, and filtrated. Then, the solvent was removed. The residue was purified by column chromatography (Hexane:Ethyl acetate = 1:1, R_f = 0.3) to obtain **7** as a white solid (17.4 g, 88%). ^{1}H NMR (300 MHz, DMSO-d_6): δ 6.87 (s, 2H), 5.12−5.08 (t, J = 6.0 Hz, 2H), 4.52−4.50 (d, J = 6.0 Hz, 4H), 3.72 (s, 3H), 3.61 (s, 3H) (the NMR spectra were in agreement with those reported).[53]

*1,3-Bis(bromomethyl)-2,5-dimethoxybenzene (**1c**).* A solution of **7** (4.0 g, 20.18 mmol) in DCM (50 mL) was cooled to 0 °C and added phosphorus tribromide (12.02 g, 44.4 mmol). The reaction mixture was allowed to warm to rt, stirred for 4 h, quenched with water (30 mL), and extracted with DCM (3 × 20 mL). The organic layers were combined, washed with brine, dried over anhydrous Na_2SO_4, and concentrated. The residue was purified by column chromatography (Hexane:DCM = 5:1, R_f = 0.35) to afford **1c** as a white solid (5.88 g, 90%). ^{1}H NMR (500 MHz, $CDCl_3$): δ 6.92 (s, 2H), 4.56 (s, 4H), 4.00 (s, 3H), 3.82 (s, 3H) (the NMR spectra were in agreement with those reported).[54]

*(2,5-Dimethoxy-1,3-phenylene)bis(methylene) Diacetate (**3a**).* A solution of **7** (0.92 g, 5 mmol) in DCM (10 mL) was added 4-dimethylaminopyridine (1.83 g, 15 mmol) and cooled to 0 °C. Then, acetyl chloride (1.57 g, 20 mmol) was added using a syringe. The reaction mixture was warmed up to rt, stirred for another 4 h, quenched with H_2O (8.0 mL), and extracted with DCM (3 × 20 mL). The organic layers were combined, washed with brine, dried over anhydrous Na_2SO_4, and concentrated. The residue was purified by

https://dx.doi.org/10.1021/acs.joc.0c02234
J. Org. Chem. XXXX, XXX, XXX−XXX

column chromatography (Hexane:Ethyl acetate = 1:1, R_f = 0.7) to obtain **3a** as a slightly yellowish liquid (1.28 g, 91%). ^{1}H NMR (300 MHz, $CDCl_3$): δ 6.90 (s, 2H), 5.15 (s, 4H), 3.78 (s, 6H), 2.11−2.10 (d, J = 3.0 Hz, 6H) [the NMR spectra were in agreement with those reported].[54] Different from the previous procedure (74% yield), 4-dimethylaminopyridine was used as a catalyst instead of pyridine, leading to a higher yield (91%)]. HRMS-ESI (+) (m/z): $[M + Na]^+$ calcd. for $C_{14}H_{18}O_6Na^+$, 305.0996; found: 305.0985.

*2,5-Dimethoxy-1,3-bis(methoxymethyl)benzene (**3b**).* To a solution of **7** (1.0 g, 5.04 mmol) in DMF (10 mL) was added NaH (605 mg, 60%, 15.12 mmol) at 0 °C. The reaction mixture was stirred at 0 °C for 10 min. Then, CH_3I (2.86 g, 20.16 mmol) was added. The reaction mixture was allowed to warm to rt, stirred for another 4 h, quenched with water (20 mL), and extracted with ethyl acetate (3 × 30 mL). The organic layers were combined, washed with brine, dried over anhydrous Na_2SO_4, and concentrated. The residue was purified by column chromatography (Hexane:Ethyl acetate = 1:1, R_f = 0.8) to obtain **3b** as a colorless liquid (1.10 g, 96%). ^{1}H NMR (500 MHz, $CDCl_3$): δ 6.92 (s, 2H), 4.51 (s, 4H), 3.81 (s, 3H), 3.76 (s, 3H), 3.44 (s, 6H). 13C{1H} NMR (125 MHz, $CDCl_3$): δ 156.0, 150.0, 132.3, 114.1, 69.4, 62.5, 58.3, 55.6. HRMS-ESI (+) (m/z): $[M + Na]^+$ calcd. for $C_{12}H_{18}O_4Na^+$, 249.1103; found: 249.1094.

*1,3-Bis((allyloxy)methyl)-2,5-dimethoxybenzene (**3c**).* A solution of **7** (1.0 g, 5.04 mmol) in DMF (10 mL) was added NaH (605 mg, 60%, 15.12 mmol) at 0 °C and stirred for 10 min. Then, allyl iodide (2.54 g, 15.12 mmol) was added. The reaction mixture was allowed to warm to rt, stirred for 3 h, quenched with water (10 mL), and extracted with ethyl acetate (3 × 30 mL). The organic layers were combined, washed with brine, dried over anhydrous Na_2SO_4, and concentrated. The residue was purified by column chromatography (Hexane:Ethyl acetate = 3:1, R_f = 0.85) to obtain **3c** as a colorless liquid (1.20 g, 86%). ^{1}H NMR (500 MHz, $CDCl_3$): δ 6.95 (s, 2H), 6.03−5.96 (m, 2H), 5.37−5.33 (d, J = 20.0 Hz, 2H), 5.24−5.22 (d, J = 10.0 Hz, 2H), 4.58 (s, 4H), 4.10−4.09 (d, J = 5.0 Hz, 4H), 3.81 (s, 3H), 3.76 (s, 3H). 13C{1H} NMR (125 MHz, $CDCl_3$): δ 156.0, 150.1, 134.8, 132.4, 117.1, 114.2, 71.4, 67.0, 62.6, 55.6. HRMS-ESI (+) (m/z): $[M + H]^+$ calcd. for $C_{16}H_{23}O_4^+$, 279.1591; found: 279.1583.

*((((2,5-Dimethoxy-1,3-phenylene)bis(methylene))bis(oxy))bis(methylene))dibenzene (**3d**).* A solution of **7** (1.0 g, 5.04 mmol) in DMF (10 mL) was cooled to 0 °C and added NaH (605 mg, 60%, 15.12 mmol). The resulting mixture was stirred for 10 min. Then, benzyl chloride (1.91 g, 15.12 mmol) was added. The reaction mixture was allowed to warm to rt, stirred for another 3 h, quenched with water (10 mL), and extracted with ethyl acetate (3 × 30 mL). The organic layers were combined, washed with brine, dried over anhydrous Na_2SO_4, and concentrated. The residue was purified by column chromatography (Hexane:Ethyl acetate = 3:1, R_f = 0.8) to afford **3d** as a colorless liquid (1.52 g, 80%). ^{1}H NMR (500 MHz, $CDCl_3$): δ 7.45−7.33 (m, 10H), 7.03 (s, 2H), 4.66 (s, 8H), 3.84 (s, 3H), 3.74 (s, 3H). 13C{1H} NMR (125 MHz, $CDCl_3$): δ 156.0, 150.2, 138.3, 132.4, 128.5, 127.9, 127.7, 114.4, 72.6, 67.1, 62.6, 62.6, 55.7, 55.6. HRMS-ESI (+) (m/z): $[M + Na]^+$ calcd. for $C_{24}H_{26}O_4Na^+$, 401.1723; found: 401.1717.

*1,1′-(2,5-Dimethoxy-1,3-phenylene)bis(N,N-dimethylmethanamine) (**3e**).* A solution of **1c** (500 mg, 1.54 mmol) in ethyl acetate (5 mL) was added dimethylamine solution (2.0 M in methanol) (3.85 mL, 7.7 mmol) and stirred at rt for 2 h. The solvent was removed. Then, water (5 mL) was added. The resulting mixture was extracted with ethyl acetate (3 × 10 mL), washed with NaOH (1.0 M), brine, and dried over anhydrous Na_2SO_4. The solvent was removed to afford **3e** as a slightly yellowish gel (350 mg, 90%). ^{1}H NMR (500 MHz, $CDCl_3$): δ 6.85 (s, 2H), 3.76 (s, 3H), 3.69 (s, 3H), 3.42 (s, 4H), 2.24 (s, 12H). 13C{1H} NMR (75 MHz, $CDCl_3$): δ 155.7, 151.1, 132.5, 114.6, 61.9, 57.9, 55.6, 45.4. HRMS-ESI (+) (m/z): $[M + H]^+$ calcd. for $C_{14}H_{25}N_2O_2^+$, 253.1911; found: 253.1905.

*4,4′-((2,5-Dimethoxy-1,3-phenylene)bis(methylene))dimorpholine (**3f**).* A solution of **1c** (324 mg, 1.0 mmol) in ethyl acetate (4 mL) was added morpholine (871 mg, 10.0 mmol), stirred at rt overnight, diluted with water (5 mL), and then extracted with ethyl acetate (3 × 10 mL). The organic phases were combined, washed with NaOH (1.0 M), brine, and dried over anhydrous Na_2SO_4. The solvent was removed to afford **3f** as a white solid (333 mg, 99%), m.p. 114−115 °C. ^{1}H NMR (500 MHz, $CDCl_3$): δ 6.92 (s, 2H), 3.81 (s, 3H), 3.78 (s, 3H), 3.74−3.72 (t, J = 5.0 Hz, 8H), 3.54 (s, 4H), 2.52 (s, 8H). 13C{1H} NMR (125 MHz, $CDCl_3$): δ 155.5, 151.5, 132.1, 114.5, 67.2, 62.2, 57.1, 55.6, 53.7. HRMS-ESI (+) (m/z): $[M + H]^+$ calcd. for $C_{18}H_{29}N_2O_4^+$, 337.2122; found: 337.2113.

*((2,5-Dimethoxy-1,3-phenylene)bis(methylene))bis(phenylsulfane) (**3g**).* A solution of **1c** (648 mg, 2.0 mmol) in DMF (10 mL) was added thiophenol (661.2 mg, 6.0 mmol) followed by trimethylamine (0.6 mL). The reaction mixture was stirred at 70 °C overnight, quenched with water (20 mL), and extracted with ethyl acetate (3 × 20 mL). The organic layers were combined, washed with brine, dried over anhydrous Na_2SO_4, and concentrated. The residue was purified by column chromatography (Hexane:ethyl acetate = 6:1, R_f = 0.4) to afford **3g** as a white solid (620 mg, 81%), m.p. 63−64 °C. ^{1}H NMR (500 MHz, $CDCl_3$): δ 7.40−7.38 (m, 4H), 7.33−7.30 (m, 4H), 7.25−7.22 (m, 2H), 6.74 (s, 2H), 4.18 (s, 4H), 3.86 (s, 3H), 3.66 (s, 3H). 13C{1H} NMR (125 MHz, $CDCl_3$): δ 155.5, 150.2, 136.5, 131.6, 129.9, 129.0, 126.4, 115.0, 62.7, 55.5, 33.3. HRMS-ESI (+) (m/z): $[M + K]^+$ calcd. for $C_{22}H_{22}O_2S_2K^+$, 421.0693; found: 421.0687.

*((2,5-Dimethoxy-1,3-phenylene)bis(methylene))bis(phenylselane) (**3h**).* A solution of diphenyl diselenide (624 mg, 2.0 mmol) in DMF (5.0 mL) was added $NaBH_4$ (151 mg, 4.0 mmol) and stirred at rt for 10 min. Then, **1c** (324 mg, 1.0 mmol) in DMF (4.0 mL) was added. The resulting mixture was stirred overnight, quenched with water (20 mL), and extracted with ethyl acetate (3 × 20 mL). The organic layers were combined, washed with brine, dried over anhydrous Na_2SO_4, and concentrated. The residue was purified by column chromatography (Hexane:DCM = 4:1, R_f = 0.5) to afford **3h** as a white solid (300 mg, 63%), m.p. 38−39 °C. ^{1}H NMR (500 MHz, $CDCl_3$): δ 7.55−7.54 (m, 4H), 7.31−7.29 (t, J = 5.0 Hz, 6H), 4.16 (s, 4H), 3.86 (s, 3H), 3.59 (s, 3H). 13C{1H} NMR (125 MHz, $CDCl_3$): δ 155.2, 149.8, 133.6, 132.9, 130.7, 129.1, 127.4, 114.9, 62.1, 55.4, 26.5. HRMS-ESI (+) (m/z): $[M + K]^+$ calcd. for $C_{22}H_{22}O_2Se_2K^+$, 516.9586; found: 516.9580.

*((2,5-Dimethoxy-1,3-phenylene)bis(methylene))bis(triphenylphosphonium) Bromide (**3i**).* A mixture of **1c** (324 mg, 1.0 mmol) and triphenylphosphine (630 mg, 2.4 mmol) in dry toluene (5.0 mL) was refluxed for 6 h under argon. The crude white powder was obtained by filtration, which was washed with ether (3 × 20 mL) to afford **3i** as a white foam (840 mg, 99%). ^{1}H NMR (500 MHz, $CDCl_3$): δ 7.79−7.62 (m, 6H), 7.67−7.64 (m, 24H), 6.53 (s, 2H), 5.18−5.15 (d, J = 15.0 Hz, 4H), 3.17 (s, 3H), 2.86 (s, 3H): m.p. 270−271 °C. 13C{1H} NMR (125 MHz, $CDCl_3$): δ 151.5, 135.3, 134.2, 134.2, 134.1, 130.5, 130.5, 130.4, 123.3, 118.1, 117.9, 117.9, 117.9, 117.4, 55.5, 26.0, 25.6. HRMS-ESI (+) (m/z): $[M - 2Br]^{2+}$ calcd. for $C_{46}H_{42}O_2P_2^{2+}$, 344.1325; found: 344.1319.

Radical Trapping with Monomers. Compound **3i** (100 mg, 0.118 mmol) in CH_3CN (1.5 mL) was added TEMPO (184 mg, 1.18 mmol) under stirring at rt. The resulting mixture was irradiated under UV (350 nm) for 5 days and concentrated. The residue was purified by chromatography (DCM:MeOH = 10:1) to afford compound **11c** as a white foam (24 mg, 31%). ^{1}H NMR (300 MHz, $CDCl_3$): δ 7.74−7.61 (m, 15 H), 6.97 (s, 1H), 6.69 (s, 1H), 5.23−5.19 (d, J = 12.0 Hz, 2H), 4.58 (s, 2H), 3.52−3.49 (d, J = 9 Hz, 6H), 1.47 (s, 4H), 1.34 (s, 2H), 1.15−1.11 (d, J = 12.0 Hz, 12H). 13C{1H} NMR (75 MHz, $CDCl_3$): δ 155.7, 155.7, 134.9, 134.4, 134.2, 130.1, 129.9, 121.1, 121.0, 118.7, 117.5, 116.5, 114.7, 72.9, 62.0, 60.0, 55.7, 39.7, 32.9, 20.7, 17.0. HRMS-ESI (+) (m/z): $[M - Br]^+$ calcd. for $C_{37}H_{45}NO_3P^+$, 582.3132; found: 582.3115.

Carbocation Trapping with Monomers. A solution of $MeONH_2$·HCl (394 mg, 4.72 mmol) in DMF (2 mL) was added trimethylamine (567 mg, 5.20 mmol) and stirred at rt for 30 min. Then, **3i** (100 mg, 0.118 mmol) in DMF (1 mL) was added. The resulting mixture was stirred for 20 min, irradiated with 350 nm light for 2 days, quenched with water, and extracted with ethyl acetate (3 × 3 mL). The combined organic phases were combined, washed with

https://dx.doi.org/10.1021/acs.joc.0c02234
J. Org. Chem. XXXX, XXX, XXX−XXX

brine, and dried over anhydrous Na_2SO_4. After removing the solvent, the residue was analyzed by LC-MS. The products were analyzed by both LC-MS and HRMS, indicating the formation of **11a** and **11b**. **11a**: HRMS-ESI (+) (m/z): $[M - Br]^+$ calcd. for $C_{28}H_{27}O_2PCl^+$, 461.1432; found: 461.1408. **11b**: HRMS-ESI (+) (m/z): $[M - Br]^+$ calcd. for $C_{29}H_{29}NO_3P^+$, 470.1880; found: 470.1839 (Note: the amount of **11a** or **11b** obtained was not sufficient to conduct NMR spectroscopic analysis due to an extremely slow and complex reaction).

ICL Assay with Duplex DNA. The ^{32}P-labeled oligonucleotide (0.5 μM) was annealed with 1.5 equiv of the complementary strand by heating to 90 °C for 5 min in potassium phosphate buffer (pH 7, 10 mM), followed by cooling to rt. The ^{32}P-labeled ODN duplex (2 μL, 0.5 μM) was then mixed with 1 M NaCl (2 μL), 100 mM potassium phosphate (2 μL, pH 8), and **3a**−**i** or **2a**−**i** (concentration range: 10 μM to 2 mM in 6 μL CH_3CN), and autoclaved distilled water to give a final volume of 20 μL. The reaction was irradiated under UV (350 nm) at room temperature until the reaction was completed followed by quenching with an equal volume of 90% formamide loading buffer. The resulting mixture was then subjected to 20% denaturing polyacrylamide gel for electrophoresis.

Trapping Assay with DNA ICL Reactions. For carbocation trapping, the stock solution of $MeONH_2{\cdot}HCl$ (2 M) was titrated with NaOH (5 M) to adjust the pH to 7.0, which was then diluted to desired concentration (1/3-1000/3 mM). A 6 μL solution of which was mixed with ^{32}P-labeled DNA duplex (2 μL, 0.5 μM), NaCl (2 μL, 1 M) potassium phosphate (2 μL, pH 8.0, 100 mM), compound (**3a**−**i** or **2a**−**i**) in 6 μL of CH_3CN (optimized concentration was used for each compound), and water (2 μL) to give the desired concentration (final $MeONH_2$ concentration: 100 μM to 100 mM). For radical trapping reaction, 3 μL of TEMPO in CH_3CN (200/3 μM to 2000/3 mM) was mixed with the following: ^{32}P-labeled DNA duplex (2 μL, 0.5 μM), NaCl (2 μL, 1 M), potassium phosphate (2 μL, pH 8.0, 100 mM), compound (**3a**−**i** or **2a**−**i**) in CH_3CN (3 μL) (optimized concentration was used for each compound), and water (8 μL) as appropriate for the desired concentration (final TEMPO concentration: 10 μM to 100 mM). The reaction mixture was irradiated with 350 nm light at room temperature for desired time (optimized time for each compound was used), quenched with an equal volume of 90% formamide loading buffer, and then subjected to 20% denaturing polyacrylamide gel electrophoresis.

Stability Study of ICL Products Formed with 8. The ^{32}P-labeled oligonucleotide duplex **8** (60 μ, 0.5 μM) was mixed with NaCl (12 μL, 1 M), 100 mM potassium phosphate (12 μL, pH 8.0) and compound (**3a**−**i** or **2a**−**i**) in CH_3CN (36 μL) (optimized concentration used for all compounds). The reaction mixture was irradiated with 350 nm light for the desired time (optimized time). After the cross-linking reaction, the DNA ICLs and the monoalkylated ODNs were purified by gel electrophoresis. The isolated DNA fragments were dissolved in 60 μL of water and divided into three portions equally. One portion was incubated with 1.0 M piperidine at 90 °C for 0.5 h, the second portion was incubated with 0.1 M NaCl and 10 mM potassium phosphate buffer (pH 7.0) under the same condition, the third portion (without treatment) was used as a control. The solvent was removed under vacuum after heating, dissolved in 90% formamide loading buffer, and then subjected to electrophoresis on a 20% denaturing polyacrylamide gel.

■ ASSOCIATED CONTENT

Supporting Information

The Supporting Information is available free of charge at https://pubs.acs.org/doi/10.1021/acs.joc.0c02234.

Experimental procedures for reactions and analysis, characterization of **1**−**11**, DNA experiments, NMR, and IT-TOF analysis (PDF)

■ AUTHOR INFORMATION

Corresponding Author

Xiaohua Peng − *Department of Chemistry and Biochemistry and the Milwaukee Institute for Drug Discovery, University of Wisconsin Milwaukee, Milwaukee, Wisconsin 53211, United States;* orcid.org/0000-0001-5627-0606; Phone: 414-229-5221; Email: pengx@uwm.edu

Author

Heli Fan − *Department of Chemistry and Biochemistry and the Milwaukee Institute for Drug Discovery, University of Wisconsin Milwaukee, Milwaukee, Wisconsin 53211, United States*

Complete contact information is available at: https://pubs.acs.org/10.1021/acs.joc.0c02234

Notes

The authors declare no competing financial interest.

■ ACKNOWLEDGMENTS

This work was supported by the Great Milwaukee Foundation (Shaw Scientist Award), the University of Wisconsin Milwaukee Research Growth Initiative, and the Wisconsin Applied Research Grant.

■ REFERENCES

(1) Brulikova, L.; Hlavac, J.; Hradil, P. DNA interstrand cross-linking agents and their chemotherapeutic potential. *Curr. Med. Chem.* **2012**, *19*, 364−385.

(2) Rajski, S. R.; Williams, R. M. DNA Cross-Linking Agents as Antitumor Drugs. *Chem. Rev.* **1998**, *98*, 2723−2796.

(3) Chen, W.; Balakrishnan, K.; Kuang, Y.; Han, Y.; Fu, M.; Gandhi, V.; Peng, X. Reactive oxygen species (ROS) inducible DNA cross-linking agents and their effect on cancer cells and normal lymphocytes. *J. Med. Chem.* **2014**, *57*, 4498−4510.

(4) Chen, W.; Fan, H.; Balakrishnan, K.; Wang, Y.; Sun, H.; Fan, Y.; Gandhi, V.; Arnold, L. A.; Peng, X. Discovery and Optimization of Novel Hydrogen Peroxide Activated Aromatic Nitrogen Mustard Derivatives as Highly Potent Anticancer Agents. *J. Med. Chem.* **2018**, *61*, 9132−9145.

(5) Noll, D. M.; Mason, T. M.; Miller, P. S. Formation and repair of interstrand cross-links in DNA. *Chem. Rev.* **2006**, *106*, 277−301.

(6) Peng, X.; Ghosh, A. K.; Van Houten, B.; Greenberg, M. M. Nucleotide excision repair of a DNA interstrand cross-link produces single- and double-strand breaks. *Biochemistry* **2010**, *49*, 11−19.

(7) Dronkert, M. L. G.; Kanaar, R. Repair of DNA interstrand cross-links. *Mutat. Res.* **2001**, *486*, 217−247.

(8) Peng, X.; Greenberg, M. M. Facile SNP detection using bifunctional, cross-linking oligonucleotide probes. *Nucleic Acids Res.* **2008**, *36*, No. e31.

(9) Sun, H.; Peng, X. Template-directed fluorogenic oligonucleotide ligation using "click" chemistry: detection of single nucleotide polymorphism in the human p53 tumor suppressor gene. *Bioconjugate Chem.* **2013**, *24*, 1226−1234.

(10) Ogasawara, S.; Fujimoto, K. SNP genotyping by using photochemical ligation. *Angew. Chem., Int. Ed.* **2006**, *45*, 4512−4515.

(11) Freccero, M. Quinone Methides as Alkylating and Cross-Linking Agents. *Mini-Rev. Org. Chem.* **2004**, *1*, 403−415.

(12) Percivalle, C.; Doria, F.; Freccero, M. Quinone Methides as DNA Alkylating Agents: An Overview on Efficient Activation Protocols for Enhanced Target Selectivity. *Curr. Org. Chem.* **2014**, *18*, 19−43.

(13) Verga, D.; Nadai, M.; Doria, F.; Percivalle, C.; Di Antonio, M.; Palumbo, M.; Richter, S. N.; Freccero, M. Photogeneration and reactivity of naphthoquinone methides as purine selective DNA alkylating agents. *J. Am. Chem. Soc.* **2010**, *132*, 14625−14637.

(14) Wang, P.; Liu, R.; Wu, X.; Ma, H.; Cao, X.; Zhou, P.; Zhang, J.; Weng, X.; Zhang, X.-L.; Qi, J.; Zhou, X.; Weng, L. A potent, water-soluble and photoinducible DNA cross-linking agent. *J. Am. Chem. Soc.* **2003**, *125*, 1116−1117.
(15) Weng, X.; Ren, L.; Weng, L.; Huang, J.; Zhu, S.; Zhou, X.; Weng, L. Synthesis and biological studies of inducible DNA cross-linking agents. *Angew. Chem., Int. Ed.* **2007**, *46*, 8020−8023.
(16) Wang, Y.; Liu, S.; Lin, Z.; Fan, Y.; Wang, Y.; Peng, X. Photochemical Generation of Benzyl Cations That Selectively Cross-Link Guanine and Cytosine in DNA. *Org. Lett.* **2016**, *18*, 2544−2547.
(17) Hong, I. S.; Greenberg, M. M. DNA interstrand cross-link formation initiated by reaction between singlet oxygen and a modified nucleotide. *J. Am. Chem. Soc.* **2005**, *127*, 10510−10511.
(18) Carrette, L. L. G.; Gyssels, E.; De Laet, N.; Madder, A. Furan oxidation based cross-linking: a new approach for the study and targeting of nucleic acid and protein interactions. *Chem. Commun.* **2016**, *52*, 1539−1554.
(19) Stevens, K.; Madder, A. Furan-modified oligonucleotides for fast, high-yielding and site-selective DNA inter-strand cross-linking with non-modified complements. *Nucleic Acids Res.* **2009**, *37*, 1555−1565.
(20) Zeng, Q.; Rokita, S. E. Tandem quinone methide generation for cross-linking DNA. *J. Org. Chem.* **1996**, *61*, 9080−9081.
(21) Veldhuyzen, W. F.; Pande, P.; Rokita, S. E. A transient product of DNA alkylation can be stabilized by binding localization. *J. Am. Chem. Soc.* **2003**, *125*, 14005−14013.
(22) Wang, H.; Wahi, M. S.; Rokita, S. E. Immortalizing a transient electrophile for DNA cross-linking. *Angew. Chem., Int. Ed.* **2008**, *47*, 1291−1293.
(23) Kuang, Y.; Balakrishnan, K.; Gandhi, V.; Peng, X. Hydrogen peroxide inducible DNA cross-linking agents: targeted anticancer prodrugs. *J. Am. Chem. Soc.* **2011**, *133*, 19278−19281.
(24) Cao, S.; Wang, Y.; Peng, X. ROS-inducible DNA cross-linking agent as a new anticancer prodrug building block. *Chem. − Eur. J.* **2012**, *18*, 3850−3854.
(25) Fan, H.; Peng, X. Novel DNA Cross-Linking Reagents. In *Advances in Molecular Toxicology*; Fishbein, J. C., Heilma, J. M., Eds.; Academic Press: 2016; *10*, pp. 235−292.
(26) Takasugi, M.; Guendouz, A.; Chassignol, M.; Decout, J. L.; Lhomme, J.; Thuong, N. T.; Hélène, C. Sequence-Specific Photo-induced Cross-Linking of the two Strands of Double-Helical DNA by a Psoralen Covalently Linked to a Triple Helix-Forming Oligonucleotide. *Proc. Natl. Acad. Sci. U. S. A.* **1991**, *88*, 5602−5606.
(27) Thazhathveetil, A. K.; Liu, S.-T.; Indig, F. E.; Seidman, M. M. Psoralen conjugates for visualization of genomic interstrand cross-links localized by laser photoactivation. *Bioconjugate Chem.* **2007**, *18*, 431−437.
(28) Kashida, H.; Doi, T.; Sakakibara, T.; Hayashi, T.; Asanuma, H. *p*-Stilbazole moieties as artificial base pairs for photo-cross-linking of DNA duplex. *J. Am. Chem. Soc.* **2013**, *135*, 7960−7966.
(29) Haque, M. M.; Sun, H.; Liu, S.; Wang, Y.; Peng, X. Photoswitchable formation of a DNA interstrand cross-link by a coumarin-modified nucleotide. *Angew. Chem., Int. Ed.* **2014**, *53*, 7001−7005.
(30) Sun, H.; Fan, H.; Peng, X. Quantitative DNA interstrand cross-link formation by coumarin and thymine: structure determination, sequence effect, and fluorescence detection. *J. Org. Chem.* **2014**, *79*, 11359−11369.
(31) Fujimoto, K.; Yamada, A.; Yoshimura, Y.; Tsukaguchi, T.; Sakamoto, T. Details of the Ultrafast DNA Photo-Cross-Linking Reaction of 3-Cyanovinylcarbazole Nucleoside:*Cis-Trans*Isomeric Effect and the Application for SNP-Based Genotyping. *J. Am. Chem. Soc.* **2013**, *135*, 16161−16167.
(32) Sakamoto, T.; Tanaka, Y.; Fujimoto, K. DNA photo-cross-linking using 3-cyanovinylcarbazole modified oligonucleotide with threoninol linker. *Org. Lett.* **2015**, *17*, 936−939.
(33) Op de Beeck, M.; Madder, A. Sequence specific DNA cross-linking triggered by visible light. *J. Am. Chem. Soc.* **2012**, *134*, 10737−10740.
(34) Richter, S. N.; Maggi, S.; Mels, S. C.; Palumbo, M.; Freccero, M. Binol quinone methides as bisalkylating and DNA cross-linking agents. *J. Am. Chem. Soc.* **2004**, *126*, 13973−13979.
(35) Chatterjee, M.; Rokita, S. E. The Role of a Quinone Methide in the Sequence Specific Alkylation of DNA. *J. Am. Chem. Soc.* **1994**, *116*, 1690−1697.
(36) Chatterjee, M.; Rokita, S. E. Inducible Alkylation of DNA Using an Oligonucleotide-Quinone Conjugate. *J. Am. Chem. Soc.* **1990**, *112*, 6397−6399.
(37) Lin, G.; Li, L. Oxidation and reduction of the 5-(2′-deoxyuridinyl)methyl radical. *Angew. Chem., Int. Ed.* **2013**, *52*, 5594−5598.
(38) Weng, L.; Horvat, S. M.; Schiesser, C. H.; Greenberg, M. M. Deconvoluting the reactivity of two intermediates formed from modified pyrimidines. *Org. Lett.* **2013**, *15*, 3618−3621.
(39) Fan, H.; Sun, H.; Peng, X. Substituents Have a Large Effect on Photochemical Generation of Benzyl Cations and DNA Cross-Linking. *Chem. − Eur. J.* **2018**, *24*, 7671−7682.
(40) Lin, Z.; Fan, H.; Zhang, Q.; Peng, X. Design, Synthesis, and Characterization of Binaphthalene Precursors as Photoactivated DNA Interstrand Cross-Linkers. *J. Org. Chem.* **2018**, *83*, 8815−8826.
(41) Wang, Y.; Lin, Z.; Fan, H.; Peng, X. Photoinduced DNA Interstrand Cross-Link Formation by Naphthalene Boronates via a Carbocation. *Chem. − Eur. J.* **2016**, *22*, 10382−10386.
(42) Weinert, E. E.; Dondi, R.; Colloredo-Melz, S.; Frankenfield, K. N.; Mitchell, C. H.; Freccero, M.; Rokita, S. E. Substituents on quinone methides strongly modulate formation and stability of their nucleophilic adducts. *J. Am. Chem. Soc.* **2006**, *128*, 11940−11947.
(43) Cao, S.; Wang, Y.; Peng, X. The leaving group strongly affects H_2O_2-induced DNA cross-linking by arylboronates. *J. Org. Chem.* **2014**, *79*, 501−508.
(44) Stupi, B. P.; Li, H.; Wang, J.; Wu, W.; Morris, S. E.; Litosh, V. A.; Muniz, J.; Hersh, M. N.; Metzker, M. L. Stereochemistry of benzylic carbon substitution coupled with ring modification of 2-nitrobenzyl groups as key determinants for fast-cleaving reversible terminators. *Angew. Chem., Int. Ed.* **2012**, *51*, 1724−1727.
(45) Zielonka, J.; Joseph, J.; Sikora, A.; Hardy, M.; Ouari, O.; Vasquez-Vivar, J.; Cheng, G.; Lopez, M.; Kalyanaraman, B. Mitochondria-Targeted Triphenylphosphonium-Based Compounds: Syntheses, Mechanisms of Action, and Therapeutic and Diagnostic Applications. *Chem. Rev.* **2017**, *117*, 10043−10120.
(46) Hong, I. S.; Ding, H.; Greenberg, M. M. Oxygen independent DNA interstrand cross-link formation by a nucleotide radical. *J. Am. Chem. Soc.* **2006**, *128*, 485−491.
(47) Hong, I. S.; Ding, H.; Greenberg, M. M. Radiosensitization by a modified nucleotide that produces DNA interstrand cross-links under hypoxic conditions. *J. Am. Chem. Soc.* **2006**, *128*, 2230−2231.
(48) Peng, X.; Hong, I. S.; Li, H.; Seidman, M. M.; Greenberg, M. M. Interstrand cross-link formation in duplex and triplex DNA by modified pyrimidines. *J. Am. Chem. Soc.* **2008**, *130*, 10299−10306.
(49) Maxam, A. M.; Gilbert, W. A new method for sequencing DNA. *Proc. Natl. Acad. Sci. U. S. A.* **1977**, *74*, 560−564.
(50) Maxam, A. M.; Gilbert, W. Sequencing end-labeled DNA with base-specific chemical cleavages. *Methods Enzymol.* **1980**, *65*, 499−560.
(51) Pittelkow, M.; Christensen, J. B.; Sølling, T. I. Substituent effects on the stability of extended benzylic carbocations: a computational study of conjugation. *Org. Biomol. Chem.* **2005**, *3*, 2441−2449.
(52) Samuel, A. P. S.; Xu, J.; Raymond, K. N. Predicting efficient antenna ligands for Tb(III) emission. *Inorg. Chem.* **2009**, *48*, 687−698.
(53) Jacques, S. A.; Michaelis, S.; Gebhardt, B.; Blum, A.; Lebrasseur, N.; Larrosa, I.; White, A. J. P.; Barrett, A. G. M. Studies on the Total Synthesis of Lactonamycin: Synthesis of the Fused Pentacyclic B−F Ring Unit. *Eur. J. Org. Chem.* **2012**, 107−113.
(54) Witiak, D. T.; Loper, J. T.; Ananthan, S.; Almerico, A. M.; Verhoef, V. L.; Filppi, J. A. Mono and bis(bioreductive) alkylating

https://dx.doi.org/10.1021/acs.joc.0c02234
J. Org. Chem. XXXX, XXX, XXX−XXX

agents: synthesis and antitumor activities in a B16 melanoma model. *J. Med. Chem.* **1989**, *32*, 1636−1642.

https://dx.doi.org/10.1021/acs.joc.0c02234
J. Org. Chem. XXXX, XXX, XXX−XXX